



# Kent Academic Repository

**Whelan, Sarah Anne (2017) *Generation and investigation of resistance mechanisms to AZD5363 in breast cancer*. Master of Science by Research (MScRes) thesis, University of Kent,.**

## Downloaded from

<https://kar.kent.ac.uk/63946/> The University of Kent's Academic Repository KAR

## The version of record is available from

## This document version

UNSPECIFIED

## DOI for this version

## Licence for this version

UNSPECIFIED

## Additional information

## Versions of research works

### Versions of Record

If this version is the version of record, it is the same as the published version available on the publisher's web site. Cite as the published version.

### Author Accepted Manuscripts

If this document is identified as the Author Accepted Manuscript it is the version after peer review but before type setting, copy editing or publisher branding. Cite as Surname, Initial. (Year) 'Title of article'. To be published in *Title of Journal*, Volume and issue numbers [peer-reviewed accepted version]. Available at: DOI or URL (Accessed: date).

### Enquiries

If you have questions about this document contact [ResearchSupport@kent.ac.uk](mailto:ResearchSupport@kent.ac.uk). Please include the URL of the record in KAR. If you believe that your, or a third party's rights have been compromised through this document please see our [Take Down policy](https://www.kent.ac.uk/guides/kar-the-kent-academic-repository#policies) (available from <https://www.kent.ac.uk/guides/kar-the-kent-academic-repository#policies>).

# Generation and investigation of resistance mechanisms to AZD5363 in breast cancer

Sarah Anne Whelan  
Biochemistry MSc

School of Biosciences  
University of Kent

Supervisor:  
Professor Michelle Garrett

University of  
**Kent**

## **Declaration**

No part of this thesis has been submitted in support of an application for any degree or qualification of the University of Kent or any other university or institute of learning.

Sarah Anne Whelan

## **Acknowledgements**

I would like to thank my supervisor Professor Michelle Garrett for her direction and guidance throughout my project, and for her help and feedback on my thesis. I also would like to thank Edith Blackburn for all of her valuable help and training in the laboratory.

I am also grateful to Edith, Nathan, Jasmine, Helen, Andy and Eithaar for their assistance and good company throughout my time in the lab – it has been a great year, and I will miss you all.

Finally, I would like to thank my parents and the rest of my family for their continued love and support this year and over the last four years of my time at university.

## Table of Contents

|   |    |
|---|----|
| Declaration .....   | 2  |
| Acknowledgements.....   | 3  |
| Abbreviations .....   | 6  |
| List of figures .....   | 8  |
| Abstract .....  | 9  |
| 1.0 Introduction .....  | 10 |
| 1.1 An introduction to cancer.....  | 10 |
| 1.2 An overview of breast cancer .....  | 10 |
| 1.3 PI3K/AKT signalling.....  | 12 |
| 1.3.1. Survival.....  | 14 |
| 1.3.2. Proliferation.....   | 14 |
| 1.3.3. Growth.....  | 14 |
| 1.4. PI3K/AKT signalling in cancer .....  | 15 |
| 1.5. PI3K/AKT inhibition in breast cancer .....                                     | 16 |
| 1.6. Resistance to cancer therapies .....   | 18 |
| 1.6.1. Drug efflux .....  | 19 |
| 1.6.2. Modification of drug targets.....  | 19 |
| 1.6.3. Drug target bypass.....  | 20 |
| 1.6.4. Resistance to PI3K/AKT pathway inhibitors .....                              | 21 |
| 1.7. Project aims and objectives.....   | 22 |
| 2.0 Materials and Methods.....  | 23 |
| 2.1. Cell lines and culture .....   | 23 |
| 2.2. Characterisation of cell line growth.....                                      | 23 |
| 2.2.1. Cell seeding density assays.....   | 23 |
| 2.2.2. GI <sub>50</sub> determination.....  | 23 |
| 2.2.3. Propidium iodide staining and flow cytometry.....                            | 24 |
| 2.3. Generation of AZD5363-resistant sub-clones .....                               | 24 |
| 2.4. Cell-based ELISA.....  | 25 |
| 2.5. Cell lysis and Western blotting.....   | 25 |
| 2.5.1. Cell lysis .....   | 25 |
| 2.5.2. BCA protein determination assay.....   | 25 |
| 2.5.3. SDS-PAGE and Western blotting.....   | 26 |
| 3.0 Results.....  | 27 |
| 3.1. Characterisation of parental cell lines .....                                  | 27 |
| 3.1.1. Cell growth characteristics .....  | 27 |
| 3.1.2. GI <sub>50</sub> determinations for T47D, MCF-7 and ZR-75-1 cell lines ..... | 31 |

|   |    |
|---|----|
| 3.1.3. Baseline signalling of parental cell lines .....   | 38 |
| 3.2. Generation and characterisation of AZD5363-resistant clones .....                                | 40 |
| 3.2.1. Determination of resistance factor in sub-clones .....   | 42 |
| 3.2.2. Determination of AKT inhibitor cross-resistance in sub-clones .....                            | 43 |
| 3.2.3. Baseline signalling in resistant sub-clones .....  | 46 |
| 3.2.4. Response of resistant sub-clones to AZD5363 .....  | 47 |
| 3.1.5. Optimisation of cell-based ELISA .....   | 49 |
| 3.3.6. Investigation of PI3K/AKT pathway signalling of resistant sub-clones by cell-based ELISA ..... | 52 |
| 4.0 Discussion .....  | 54 |
| 4.1. Introduction .....   | 54 |
| 4.2. Characterisation of sensitive breast cancer cell lines .....                                     | 54 |
| 4.3. Generation of resistant cell lines .....   | 56 |
| 4.4. Characterisation of resistant sub-clones .....   | 59 |
| 4.4.1. Determining fold-resistance to AZD5363 .....   | 59 |
| 4.4.2. Resistant sub-clones do not exhibit cross-resistance to other AKT inhibitors ..                | 59 |
| 4.4.3. PI3K/AKT signalling is not significantly altered in resistant sub-clones .....                 | 60 |
| 4.5. Development of cell-based ELISA .....  | 61 |
| 4.6. Clinical implications .....  | 62 |
| 4.7. Proposed resistance mechanism .....  | 63 |
| 4.8. Future experiments .....   | 63 |
| 4.9. Conclusions .....  | 64 |
| References .....  | 65 |

## Abbreviations

|                  |  |
|------------------|--|
| µg               | Microgram  |
| µl               | Microlitre   |
| µM               | Micromolar   |
| 4EBP1            | Eukaryotic translation initiation factor 4E binding protein 1          |
| ATP              | Adenosine triphosphate   |
| BCA              | Bicinchoninic acid   |
| BrdU             | 5-bromo-2'-deoxyuridine  |
| BSA              | Bovine serum albumin   |
| C                | Celsius  |
| cAMP             | Cyclic adenosine monophosphate   |
| CDK              | Cyclin-dependent kinase  |
| CKI              | CDK inhibitor  |
| CO <sub>2</sub>  | Carbon dioxide   |
| C-terminal       | Carboxy-terminal   |
| DMEM             | Dulbecco's modified Eagle's medium                                     |
| DMSO             | Dimethyl sulfoxide   |
| ECL              | Enhanced chemiluminescence   |
| EDTA             | Ethylenediaminetetraacetic acid  |
| EGFR             | Epidermal growth factor receptor                                       |
| ERK              | Extracellular signal-related kinase                                    |
| FBS              | Foetal bovine serum  |
| GSK3β            | Glycogen synthase kinase-3β  |
| H <sub>2</sub> O | Water  |
| HER2             | Human epidermal growth factor receptor 2                               |
| HRP              | Horseradish peroxidase   |
| IC <sub>50</sub> | Half-maximal inhibitory concentration                                  |
| kDa              | Kilo Dalton  |
| mTOR             | Mammalian target of rapamycin  |
| N-terminal       | Amino-terminal   |
| OD               | Optical density  |
| OPD              | o-phenylenediamine dihydrochloride                                     |
| PBS              | Phosphate-buffered saline  |
| PDK1             | Phosphoinositide dependent kinase 1                                    |
| PH               | Pleckstrin homology domain   |
| PI3K             | Phosphoinositide-3-kinase  |
| PIK3CA           | Phosphatidylinositol 4,5-bisphosphate 3-kinase catalytic subunit alpha |
| PIP <sub>2</sub> | Phosphatidylinositol 4,5-bisphosphate                                  |
| PIP <sub>3</sub> | Phosphatidylinositol-3,4,5-trisphosphate                               |
| PKA              | cAMP-dependent protein kinase  |
| PKB              | Protein kinase B   |
| PKC              | Protein kinase C   |

|          |  |
|----------|--|
| PKG      | cGMP-dependent protein kinase                              |
| PTEN     | Phosphatase and tensin homolog                             |
| PVDF     | Polyvinylidene fluoride                                    |
| ROCK     | Rho-associated coiled-coil kinase                          |
| RPM      | Revolutions per minute                                     |
| RTK      | Receptor tyrosine kinase                                   |
| SDS-PAGE | Sodium dodecyl sulphate polyacrylamide gel electrophoresis |
| siRNA    | Small interfering ribonucleic acid                         |
| SRB      | Sulforhodamine B   |
| TBST     | Tris-buffered saline, 0.1% Tween20                         |
| TCA      | Trichloroacetic acid                                       |
| WHO      | World Health Organisation                                  |

## List of figures

Figure 1.1. Simplified diagram of the PI3K/AKT pathway.

Figure 1.2. Chemical structure of AZD5363, with potency and selectivity against AGC kinase family members, including AKT isoforms.

Figure 2.3. Schematic diagram of three examples of drug resistance mechanisms.

Figure 2.1 – Flow diagram describing protocol of generating AZD5363-resistant clones.

Figure 3.1. Brightfield microscopy images of breast cancer cell lines in culture.

Figure 3.2. Seeding density assays of (A) MCF-7, (B) T47D, and (C) ZR-75-1 cells.

Figure 3.3. Cell viability curves of breast cancer cell lines treated with AZD5363, determined by SRB assay as a percentage of untreated controls.

Figure 3.4. Summary of  $GI_{50}$  values for AZD5363 in human breast cancer cell lines T47D, MCF-7 and ZR-75-1.

Figure 3.5. Investigation of growth of T47D cells when treated with a range of concentrations of AZD5363 over time.

Figure 3.6. Cell cycle analysis of T47D treated with AZD5363.

Figure 3.7. Western blotting of parental cell lines to assess baseline signalling.

Figure 3.8. Brightfield microscopy images of AZD5363-resistant ZR-75-1 clones in culture.

Figure 3.9. SRB assays of resistant clones treated with AZD5363 to determine fold-resistance.

Figure 3.10. SRB assays of resistant clones treated with A) MK-2206 and B) GDC0068.

Figure 3.11.  $GI_{50}$  values for AKT inhibitors in the ZR-75-1 parental and resistant clones B9 and D2.

Figure 3.12. Western blotting of untreated parental ZR-75-1 cell lines and AZD5363-resistant sub-clones B9 and D2 to assess baseline signalling.

Figure 3.13. Dose-response Western blot of ZR-75-1 parental and sub-clones, treated with 50 nM and 150 nM AZD5363 (1x and 3x  $GI_{50}$  respectively).

Figure 3.14. Optimisation of GSK3 $\beta$  cell-based ELISA using Europium and OPD substrates.

Figure 3.15. Optimisation of S6RP cell-based ELISA using Europium and OPD substrates.

Figure 3.16. Cell-based ELISA of parental ZR-75-1 and sub-clones B9 and D2.

## Abstract

The PI3K/AKT pathway is a key regulator of proliferation, growth and survival in mammalian cells and aberrations in the components of this pathway are often implicated in malignancy. In particular, mutations in this pathway are frequently responsible for the development of breast, prostate, and ovarian cancers. The high frequency of deregulation in this pathway means it represents a good therapeutic target, and there are now several AKT inhibitors in Phase II clinical trials for breast cancer, including the ATP-competitive AKT inhibitor AZD5363. Despite the initial success of many molecularly targeted drugs, acquired resistance is an emerging issue, and resistance mechanisms to AKT inhibitors are still relatively unknown. Research into resistance to CCT129254 (a precursor of AZD5363) in the A2780 ovarian cancer cell line has been previously undertaken (Akan, Jakubowski, Garrett; unpublished), revealing a reduction in 4EBP1 and increased phosphorylation of p70S6K. The aim of this project was therefore to develop breast cancer cell line models of acquired resistance to AZD5363, and investigate how these resistance mechanisms compare in the two different disease types.

Breast cancer cell lines with mutations causing upregulation in the PI3K/AKT pathway were selected for analysis and characterised for their response to AZD5363. Resistant clones were generated through limiting dilution and chronic exposure to twice the  $GI_{50}$  of AZD5363. Characterisation of parental cell lines T47D, MCF-7, and ZR-75-1 showed  $IC_{50}$  values of 0.92, 1.34, and 0.05  $\mu$ M respectively for AZD5363. Sub-clones B9 and D2 were generated from ZR-75-1, with 7.3 and 5.8-fold resistance to AZD5363, respectively. However, there was no significant cross-resistance to other AKT inhibitors GDC0068 and MK2206, and Western blotting revealed no significant changes in PI3K/AKT signalling. Taken together, this suggests that the resistance mechanism is not proximal to AKT, and another pathway may be responsible for the resistant phenotype. Additionally, a new and innovative cell-based ELISA was developed to investigate cellular signalling of GSK3 $\beta$  and S6RP as an alternative to Western blotting.

In conclusion, characterisation of AKT inhibitor-sensitive breast cancer cell lines has led to generation of resistant cell line models for AZD5363. However, these novel findings showing a lack of AKT inhibitor cross-resistance and no significant changes in PI3K/AKT signalling in these models suggests the resistance mechanism is not proximal to AKT. Therefore, the novel resistance mechanisms observed in these breast cancer cell line models are not the same as that observed in the ovarian carcinoma model. Further investigation will be required to determine the pathway responsible for acquired resistance to AZD5363 in breast cancer cells.

## **1.0 Introduction**

### **1.1 An introduction to cancer**

The American Cancer Society defines cancer as a disease characterised by the spread and uncontrolled growth of abnormal cells. These abnormal cells then invade other tissues and organs, causing irreparable damage. Oncogenesis is a multi-step process caused by genomic changes; these include dominant gain-of-function mutations in oncogenes and loss-of-function mutations in tumour suppressor genes. These mutations can be attributed to external factors such as tobacco, viruses and radiation, or to internal factors such as hereditary mutations (Hanahan and Weinberg, 2000).

Cancer represents a large disease burden and is responsible for 13% of deaths worldwide (Ferlay *et al.*, 2015). The World Health Organisation (WHO) states that out of over 100 different types of cancer lung, prostate, and colorectal cancers are the most common in males whilst breast, colorectal and lung cancers are most common in females. Additionally, current estimates expect there to be a 70% rise in new cancer cases in the next 20 years (Siegel *et al.*, 2014). These figures represent a large public health risk, therefore there is currently an intense research effort worldwide.

### **1.2 An overview of breast cancer**

Breast cancer is the most prevalent cancer worldwide, and the most common cancer in the United Kingdom. The average woman has a 1 in 8 risk of developing breast cancer in her lifetime, and there are an estimated 4.4 million women worldwide who have been diagnosed with breast cancer in the last 5 years (Parkin *et al.*, 2005). Prevalence of this disease is high, and incidence rates are still increasing. Current estimates approximate that incidence rates have annually increased by 0.5% since 1990 (Maxwell Parkin *et al.*, 2001). Therefore, breast cancer represents a significant disease burden worldwide. Despite this, prognosis is generally positive, with the average 10-year survival rate in the UK at 78%. However, developing countries remain behind at an average of 57%. In developed countries, these favourable prognoses are largely a result of early diagnosis through screening programmes, in addition to better understanding of the disease and improved treatment regimens.

There are several different schemes used in order to fully classify breast cancers. These include: histological grading, stage, and receptor expression status. For example, grading in histopathology involves assigning a numerical grade from 1 to 3 according to the degree of abnormality of the tumour cells. Tumour cells that appear phenotypically similar to that of normal cells are classified as Grade 1 and are usually slow-growing and minimally invasive. On the other hand, Grade 3 tumours are poorly differentiated in that they no longer resemble

the original tissue, spread rapidly, and are associated with poor prognoses (Elston and Ellis, 2002). Additionally, the most commonly used system to stage breast cancer is the tumour, node, and metastasis (TNM) staging system. This involves assigning a stage to each characteristic of the disease i.e. tumour size (T), presence of tumour spread to the lymph nodes (N) around the chest and neck, as well as evidence of metastasis (M) to other parts of the body. Each characteristic is assigned a number, with larger tumours, spread to lymph nodes, and metastasis all corresponding to higher numbers and a more advanced stage. For example, stage 0 is classified as a pre-cancerous condition such as ductal or lobular carcinoma in situ whereas stage 4 indicates metastatic disease (Veronesi *et al.*, 2009). Finally, classification of breast cancers into subtypes according to their receptor expression is highly important when selecting treatments, as cells that overexpress a particular receptor can be targeted with specific drugs. Hormone-receptor positive tumours can overexpress oestrogen and/or progesterone receptors and grow in response to these hormones, making them susceptible to hormone therapies such as tamoxifen which prevents oestrogen binding to its receptor. Tumours overexpressing human epidermal growth factor receptor 2 (HER2) can also be targeted with the monoclonal antibody trastuzumab to prevent tumour growth through growth factor signalling. On the other hand, 10-15% of breast cancers do not express oestrogen, progesterone, or HER2 receptors and are classified as the 'triple negative' subtype. Due to the lack of drug-sensitive targets in this subtype, it is associated with the worst prognostic outcomes (Dawood *et al.*, 2010).

Standard treatment for breast cancers caught early usually consist of breast-conserving surgery such as a lumpectomy, whereas more advanced disease may require total mastectomy. These procedures are usually followed by radiotherapy/chemotherapy to treat any undetected disease, which frequently occurs in local lymph nodes or any residual breast tissue (Ceilley *et al.*, 2005). However, such conventional treatments are limited by high toxicity to both cancerous cells and normal tissue (with associated side effects), and acquired resistance. The elucidation of molecular agents responsible for driving the proliferation of many cancers has created many novel therapeutic targets, allowing the development of drugs against specific cellular signalling pathways. This is therefore thought to decrease harmful cytotoxic side effects and increase the efficacy of treatment. Genetic deregulation of components of the phosphoinositide-3-kinase/AKT pathway is frequently associated with breast cancer, and these abnormalities represent a significant target for development of novel therapeutic agents. AZD5363 is one such targeted drug which inhibits AKT, a common driver of malignancy (Samuels *et al.*, 2004).

### 1.3 PI3K/AKT signalling

Initially identified as a result of research into insulin receptor signalling in the 1980s, the PI3K/AKT pathway is highly conserved. It is responsible for regulating many fundamental processes such as cell proliferation, survival, and resistance to apoptosis (Hennessy *et al.*, 2005). It is a tightly regulated multi-step process activated by growth factor signalling and subsequent activation of receptor tyrosine kinases (RTKs). Features of this pathway such as potent driving of tumorigenesis and the ability to be activated through interactions between Ras and PI3K have led to the completion of the current model of this pathway.

Growth factor receptors such as HER2 and EGFR act as the initial activation steps of the PI3K/AKT pathway. Ligand-mediated activation of RTKs by growth factors stimulates autophosphorylation of the RTK cytoplasmic domain, leading to activation of the catalytic subunit of PI3K known as p110 $\alpha$  (encoded by the *PIK3CA* gene). RTKs can additionally activate PI3K indirectly through activation of Ras at the plasma membrane (figure 1.1).

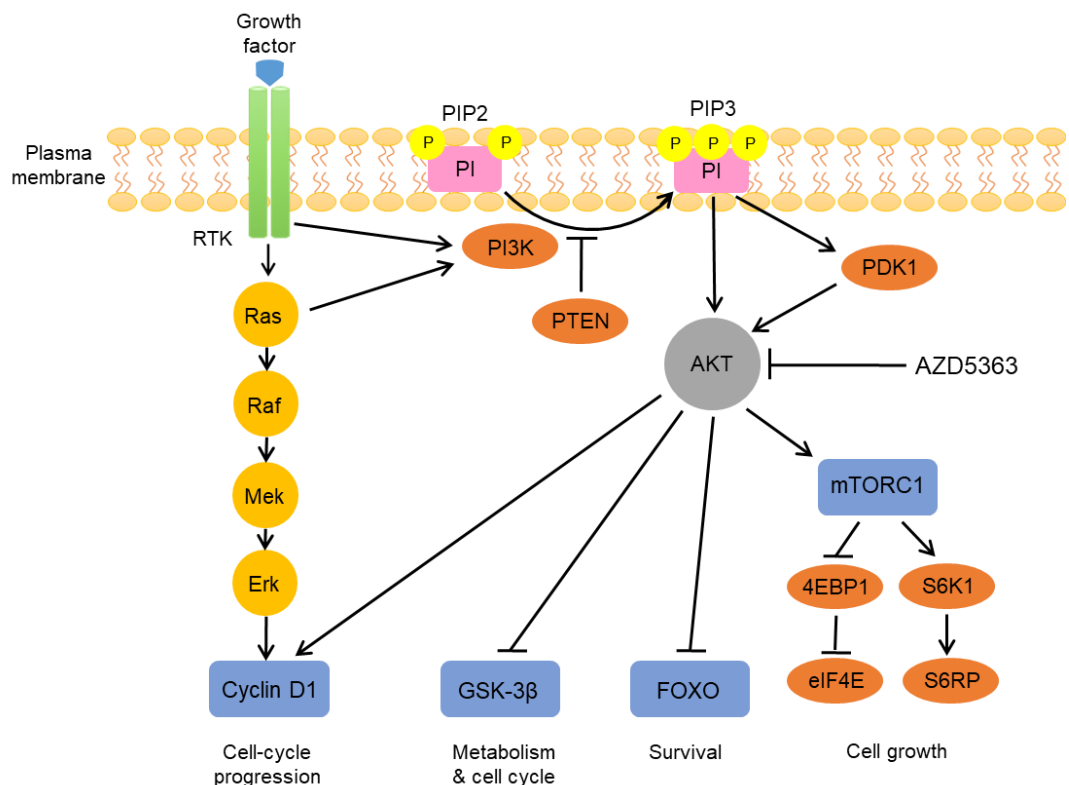


**Figure 3.1. Simplified diagram of the PI3K/AKT pathway.** Inappropriate activation of this pathway frequently leads to oncogenesis through deregulated cell-cycle progression, metabolism, and survival. Inhibition of AKT by AZD5363 is also shown.

Once PI3K has been activated, its primary role is to phosphorylate phosphoinositides in the inner leaflet of the plasma membrane, forming phosphatidylinositol-3,4,5-trisphosphate (PIP3) from phosphatidylinositol 4,5-bisphosphate (PIP2). The resulting phosphoinositols recruit AKT to the plasma membrane by binding to the Pleckstrin homology domain (PH) of AKT with high affinity. However, the presence of both PIP2 and PIP3 is required for maximal activation (Nandini, Pradip and Brian, 2017). Once bound at the plasma membrane, AKT is activated through phosphorylation of residues Thr308 and Ser473 by phosphoinositide dependent kinase 1 (PDK1) and mammalian target of rapamycin complex 2 (mTORC2), respectively (Sarbasov *et al.*, 2005; O'Reilly *et al.*, 2006). Therefore, in the absence of growth factors, AKT is not recruited to the membrane due to a lack of formation of the second messenger PIP3 – and AKT remains inactive in the cytoplasm. Activation of AKT is also negatively regulated by the tumour suppressor phosphatase and tensin homolog (PTEN), through dephosphorylation of PIP3 into PIP2 (O'Neill, Niederst and Newton, 2013).

AKT is the main signalling node of the PI3K/AKT pathway as it exerts a wide range of effects on the cell through phosphorylation of as many as 100 different substrates (Carracedo and Pandolfi, 2008). It is a member of the AGC family of kinases which includes other cytoplasmic serine/threonine kinases such as PKA, PKC, and PKG, whose activity is regulated by secondary messengers such as cyclic adenosine monophosphate (cAMP). In the case of AKT, formation of PIP3 in the plasma membrane serves as the second messenger. Additionally, there are three human isoforms of AKT known as AKT1, AKT2, and AKT3. Despite each isoform being encoded by a separate gene, these proteins all share a highly conserved structure featuring an N-terminal PH domain, a central kinase domain, and a C-terminal regulatory domain. Studies using knockdown models of each isoform have identified each as being differentially expressed in various tissues, leading to distinct physiological effects *in vivo* (Dummler and Hemmings, 2007). For example, AKT1 is expressed ubiquitously whilst AKT2 is highly expressed in adipose, liver, and skeletal muscle tissues, and AKT3 is abundantly expressed in the brain (Yu, Littlewood and Bennett, 2015). After phosphorylation and activation of AKT it is unclear how downregulation occurs, as an AKT-specific phosphatase has yet to be identified. However, exposing cells to phosphatase inhibitors results in increased the activity and phosphorylation of AKT, suggesting an as yet unknown alternative method of downregulation (Andjelkovic *et al.*, 1996).

After activation AKT has many pleiotropic effects through phosphorylation of a wide range of substrates. These cellular functions include (but are not limited to): survival, proliferation, cell growth, glucose metabolism, and protein translation.

### **1.3.1. Survival**

Signalling downstream of AKT has an important role in apoptosis and cell survival. Apoptosis is a process of programmed cell death, in which a series of biochemical events lead to changes in morphology and cell death. Such changes include: DNA fragmentation, chromatin condensation, and cell shrinkage. However, apoptosis is a fundamental process for life; for example, it is fundamental during embryonic development for correct organisation of tissues. As a result, apoptosis is a tightly regulated process, and can be negatively regulated through PI3K/AKT signalling. AKT functions in a multifactorial anti-apoptotic manner by directly phosphorylating several apoptotic components such as BAD, a member of the BCL2 family. Furthermore, AKT acts to phosphorylate and inactivate the pro-death protease caspase-9, as well as the Forkhead transcription factor FKHR to reduce transcription of pro-apoptotic proteins such as FAS ligand (Cardone, 1998). AKT can also indirectly regulate activity of the tumour suppressor p53 to prevent apoptosis through phosphorylating its negative regulator MDM2. This p53-binding protein can be phosphorylated by AKT resulting in efficient translocation to the nucleus where it labels p53 for proteasomal degradation through intrinsic E3 ubiquitin ligase activity.

### **1.3.2. Proliferation**

Furthermore, AKT plays a role in cellular proliferation through interactions with complexes that affect progress through the cell cycle. For example, components such as cyclin-dependent kinases (CDKs) and CDK inhibitors (CKIs) are essential for regulation of cell-cycle machinery. AKT functions to regulate the degradation of cyclin D1, which plays an important role in G1/S phase transition. AKT phosphorylates and thereby inactivates glycogen synthase kinase-3 $\beta$  (GSK3 $\beta$ ), a potent cyclin D1 kinase, to block its kinase activity. When cyclin D1 is phosphorylated by GSK3 $\beta$  it is degraded by the proteasome – therefore when GSK3 $\beta$  is directly phosphorylated by AKT cyclin D1 is able to accumulate and stimulate G1/S phase transition (Diehl *et al.*, 1998).

### **1.3.3. Growth**

AKT has also been suggested to play an important role in synthesis of macromolecules and cell growth. The mammalian target of rapamycin (mTOR) is a serine/threonine kinase that regulates protein synthesis, and has become known as the main regulator of cell growth. mTOR functions by activating p70 S6 kinase (an enhancer of 5' polypyrimidine mRNA translation) and inhibiting 4EBP1 (an mRNA translation repressor). Phosphorylation of eIF4E binding protein 1 (4EBP1) by mTORC1 prevents binding and subsequent inactivation of eIF4E by 4EBP1. Therefore, the unbound eIF4E is able to initiate cap-dependent

translation through the recruitment of 40S ribosomal subunits to the 5' end of mRNA. This is important as mTOR is an important substrate downstream of AKT, allowing PI3K/AKT pathway signalling to influence cell growth (Nave *et al.*, 1999).

#### **1.4. PI3K/AKT signalling in cancer**

As the signalling from these substrates are vital to survival during stressful conditions, PI3K/AKT activity is particularly important in the tumour microenvironment due to unfavourable low pH and hypoxic conditions (Datta, Brunet and Greenberg, 1999). In cancer, the PI3K/AKT pathway is frequently inappropriately activated through overexpression of activating receptors (i.e. EGFR, VEGFR), activating *PIK3CA* mutations, deleterious PTEN mutations, and hyperactivation/overexpression of AKT (Li *et al.*, 2013). Activating mutations in this pathway may result in AKT being constitutively switched "ON", and its effects on cell survival and protein synthesis can lead to oncogenesis. Such abnormalities in this pathway commonly occur in hormone receptor-positive breast cancers (Stemke-Hale *et al.*, 2008). The most common mutation in AKT itself is an E17K substitution which leads to its constitutive activation. This particular point mutation accounts for 89% of the mutations in this gene (Davies *et al.*, 2015). Similarly, tumour suppressors such as phosphatase and tensin homolog (PTEN) may also be inactivated and result in malignancy. This is because in the PI3K/AKT pathway, PTEN is a phosphatase responsible for dephosphorylating PIP3 to PIP2, thereby decreasing AKT activation. PTEN therefore acts as a negative regulator of AKT activation, responsible for maintaining homeostasis of the PI3K-Akt-mTOR signalling pathway. Additionally, inositol polyphosphate-4-phosphatase type II B (INPP4B) also has a role as a negative regulator as it catalyses hydrolysis of phosphates at position 4 of PIP3 and PIP2. The resulting products are therefore unable to bind to the PH domain of AKT also leading to reduced activation. Mutations in these phosphatases can result in AKT being constitutively active through the lack of a negative regulator, and inactivating mutations in these tumour suppressor genes are frequently found in breast cancer patients (Stambolic *et al.*, 1998). Additionally, mutations resulting in hyperactivity/overexpression of AKT are thought to mediate resistance to radiotherapy and chemotherapy, and are also associated with poor prognosis (Cheng *et al.*, 2005).

Sources of inappropriate signalling of the PI3K/AKT pathway may include somatic activating mutations or overexpression of genes encoding key components of the pathway. For example, PI3K activity is precisely regulated either directly or indirectly by ligand binding to receptor tyrosine kinases (RTKs) such as human epidermal growth factor receptor 2 (HER2). HER2 has the strongest kinase activity over all other family members, and is subsequently found overexpressed in 25-30% of all invasive breast and ovarian cancers,

with a generally poor prognosis (Moasser, 2007). Moreover, constitutive kinase activity of PI3K is found in 27% of breast cancers, resulting from mutations in a conserved area of the gene *PIK3CA* which encodes the catalytic subunit of PI3K known as p110 $\alpha$  (Samuels *et al.*, 2004). Mutations in *PIK3CA* can also co-occur with mutations conferring PTEN loss, with an observed frequency of 8.7% in breast cancers (Saal *et al.*, 2005).

As a result of these aberrations which drive malignancy, PI3K pathway inhibitors (particularly those targeting AKT) are now widely regarded as a promising focus for molecularly targeted cancer therapies, especially for breast cancer (Liu *et al.*, 2009; Zhang *et al.*, 2016). In the future, the presence of these aberrations may be used for patient stratification to ensure patients receive the appropriate therapeutics specific to their particular disease.

### **1.5. PI3K/AKT inhibition in breast cancer**

There are currently many novel small molecules in development to target components of the PI3K/AKT/mTOR pathway for the treatment of cancer. Many of these molecular targeted drug candidates have been discovered through fragment-based screening and structure-based drug design. This process involves screening large numbers of low molecular weight compounds capable of binding to the target of interest with low affinity. Compounds are selected from this pool and optimised to bind with high affinity and selectivity, and the binding characteristics analysed through techniques such as NMR or X-ray crystallography (Kumar, Voet and Zhang, 2012).

AZD5363 is a potent novel pyrrolopyrimidine derivative ATP-competitive AKT inhibitor discovered through this method (see figure 1.2). This compound has been shown to reduce cell proliferation *in vitro* through inhibition of AKT kinase activity (Zhang *et al.*, 2016). Furthermore, it also inhibits growth of human tumour xenografts in breast cancer models, both as a monotherapy and when given in combination with drugs such as trastuzumab, paclitaxel and docetaxel. Isolated enzyme assays have demonstrated that AZD5363 is a pan-AKT inhibitor, capable of potently inhibiting human AKT isoforms AKT1, AKT2, and AKT3. Furthermore, when tested in an enzyme panel consisting of 75 kinases, significant activity (defined as >75% inhibition at 1  $\mu$ M of the drug) was seen in 15 kinases – 14 of which were other members of the AGC kinase family (Addie *et al.*, 2013).

| Kinase | IC <sub>50</sub> (nM) |
|--------|-----------------------|
| AKT1   | 3                     |
| p70S6K | 6                     |
| PKA    | 7                     |
| AKT2   | 8                     |
| AKT3   | 8                     |
| ROCK2  | 60                    |
| ROCK1  | 470                   |

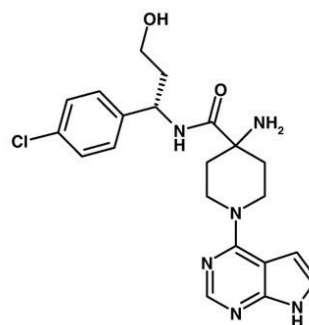


**Figure 1.2. Chemical structure of AZD5363, with potency and selectivity against AGC kinase family members, including AKT isoforms.** Table adapted from Addie *et al.* 2013, chemical structure from Davies *et al.* 2012.

The inhibition of AKT by compounds such as AZD5363 has many significant downstream effects. For example, phosphorylation of FOXO3a is prevented, allowing it to translocate into the nucleus and initiate transcription of genes associated with apoptosis. AZD5363 has also shown to increase phosphorylation of AKT itself. This is consistent with findings from other studies of ATP-competitive AKT inhibitors, as the ATP binding site of the kinase is occupied although it is catalytically inactive (Okuzumi *et al.*, 2009). This is thought to be due to conformational changes induced by occupation of the ATP binding pocket, preventing access of phosphatases to the phosphorylation sites. From a panel of 182 cell lines 41 were identified as sensitive to AZD5363, 25 of which were identified to be ‘highly sensitive’ with an GI<sub>50</sub> of <1 μmol/L. Such cell proliferation assays revealed that cell lines with mutations in PIK3CA, PTEN, or HER2 amplification displayed the highest sensitivity (Davies *et al.*, 2012).

AZD5363 is currently in Phase II clinical trials to assess antitumour activity in solid tumours bearing mutations in Akt1, PIK3CA, or PTEN (study NCT01226316). Data from a previous phase I study showed that AZD5363 was well tolerated in patients with solid tumours following both intermittent and continuous dosing schedules, although intermittent dosing was generally more tolerable. The most frequently observed adverse events included diarrhoea, hyperglycaemia, and nausea – however, preliminary evidence of antitumour effects were also observed (Tamura *et al.*, 2016). Hyperglycaemia is a common side effect of inhibition of the PI3K/AKT/mTOR pathway due to its role in insulin function and glycogen synthesis – providing proof of principle for PI3K/AKT pathway inhibition (Crouthamel *et al.*,

2009). Maximum tolerated dose (MTD) observed in one Western study was 320 mg for a continuous schedule, and 480 mg for an intermittent schedule (4 days on, 3 days off). This study showed promising activity of AZD5363 as a single agent, leading to support in further combined studies (Banerji *et al.*, 2015). Furthermore, pre-clinical studies have demonstrated a synergistic effect with the addition of AZD8931, an inhibitor of EGFR/HER2/HER3 signalling. This causes combined inhibition of the PI3K and ERK pathways, resulting in increased cell death *in vitro* and significant tumour regression *in vivo*. These findings also revealed that HER2-amplified cell lines were particularly sensitive to these synergistic effects (Crafter *et al.*, 2015). Similarly, low PTEN expression is correlated with poor response to trastuzumab, leading to the possibility of using AKT inhibitors to treat this kind of disease (Nagata *et al.*, 2004).

Two other AKT inhibitors are also under evaluation in clinical trials; GDC0068 and MK-2206. GDC0068 (also known as ipatasertib) is another ATP-competitive inhibitor of all three AKT isoforms. It has been shown to be effective as a single agent in xenograft models with aberrations in the PI3K/AKT pathway (Lin *et al.*, 2013), as well as inducing tumour regression when combined with docetaxel (Lin *et al.*, 2013). MK-2206 is a highly potent and selective AKT inhibitor due to its allosteric mechanism of action. This small molecule binds to AKT in a pocket formed between the kinase domain and the PH domain, thereby maintaining the kinase in its inactive conformation. It has demonstrated synergy when paired with cytotoxic chemotherapies such as doxorubicin, erlotinib and lapatinib, suggesting a viable clinical use for this compound (Hirai *et al.*, 2010).

In addition to AKT inhibitors, the inhibitors of this pathway that are currently in the most advanced stages of development are inhibitors of PI3K. For example, idelalisib is a selective PI3K $\delta$  inhibitor and the first to be approved by the US Food and Drug Administration (FDA) and European Medicines Agency (EMA) for treatment of haematological malignancies such as chronic lymphocytic leukaemia (Yang *et al.*, 2015). There are also several inhibitors still in development such as buparlisib and alpelisib, which have already demonstrated reasonable efficacy in preclinical models (Maira *et al.*, 2012; Fritsch *et al.*, 2014).

## **1.6. Resistance to cancer therapies**

Despite there being many benefits to the development of novel molecular targeted therapies such as AZD5363, a significant downside of their use is that many tumours readily become resistant to them. The therapeutic efficacy of these drugs is therefore reduced, as they are generally limited to use in patients with mutations in these specific targets and the effects are limited to the short term due to resistance (Spaans and Goss, 2014). For these reasons,

molecular targeted therapies are generally most effective when paired with at least one other targeted therapy, or with more traditional broad-spectrum cytotoxic chemotherapy drugs. Furthermore, resistance to these agents is manifested in two different ways: intrinsic and acquired resistance. Cancer cells that are intrinsically resistant to certain therapies have an innate characteristic at the time of diagnosis meaning they do not initially respond to the drug. On the other hand, most molecular targeted therapies are often rendered ineffective through acquired resistance, despite an initial response in the patient to the drug. There are many mechanisms that cause drug resistance – these include: drug efflux, modification of the drug target, activation of signals up- or downstream of the target, altered drug metabolism, and bypass of the drug target. The degree of heterogeneity within tumours has also become an increasingly important topic, as it has been proposed that acquired resistance may arise through positive selection of small populations of resistant cells present in the original tumour as a result of drug therapy (Swanton, 2012).

### **1.6.1. Drug efflux**

Promotion of efflux of drugs from the cell through membrane transporter proteins has also been linked to resistance to common chemotherapeutic agents. Three members of the ATP-binding cassette (ABC) family of membrane transporters have been extensively studied in the context of multi-drug resistance (MDR): multi-drug resistance protein 1 (MDR1), MDR-associated protein 1 (MRP1), and breast cancer resistance protein (BCRP). All three transporters promote the efflux of frequently used classes of chemotherapeutic agents such as taxanes, topoisomerase inhibitors, and antimetabolites. For example, MDR1 is abundantly expressed in excretory tissues such as the colon and small intestine, and has been found to cause both acquired and intrinsic resistance in tumours due to overexpression of the transporter and subsequent increase in efflux of chemotherapeutic agents (Thomas and Coley, 2003).

### **1.6.2. Modification of drug targets**

Firstly, genes encoding specific drug targets can become mutated, leading to changes in the protein product. Kinases are often responsible for oncogenesis, and mutations in these enzymes can limit the ability of the drug to inhibit the kinase, otherwise known as a 'gatekeeper' mutation. For example, approximately 50% of non-small cell lung cancer patients with activating epidermal growth factor receptor (EGFR) mutations treated with EGFR inhibitors (such as gefitinib and erlotinib) display a T790M mutation in *EGFR*. This gatekeeper mutation is responsible for acquired resistance to these agents, and can render these therapies ineffective within just one year of treatment (Yu *et al.*, 2013).

### 1.6.3. Drug target bypass

The process of oncogenic bypass is of particular importance due to its role in acquired resistance to new molecularly targeted drugs, particularly the well-known example of the mutant BRAF inhibitor vemurafenib. Oncogenic bypass occurs when other kinases distinct from the drug target can become activated (either through altered feedback pathways or selectivity of cells with appropriate genetic mutations) despite the drug still being effective in inhibiting the target kinase, creating a redundancy in the signalling pathway. Cancer patients (particularly those with melanoma) with an activating V600E mutation in *BRAF* have initially high response rates when treated with the BRAF<sup>V600E</sup> inhibitor vemurafenib – however, resistance can rapidly develop as a result of oncogenic bypass. Several mechanisms have been identified, including compensatory activation of other RAF isoforms and positive selection of subpopulations of tumour cells with mutations in other components of the pathway such as *KRAS* and *NRAS* (Nazarian *et al.*, 2010a). Additionally, upregulation of the PI3K/AKT pathway through mutations was observed in 22% of cases with acquired resistance to vemurafenib (Shi *et al.*, 2014).

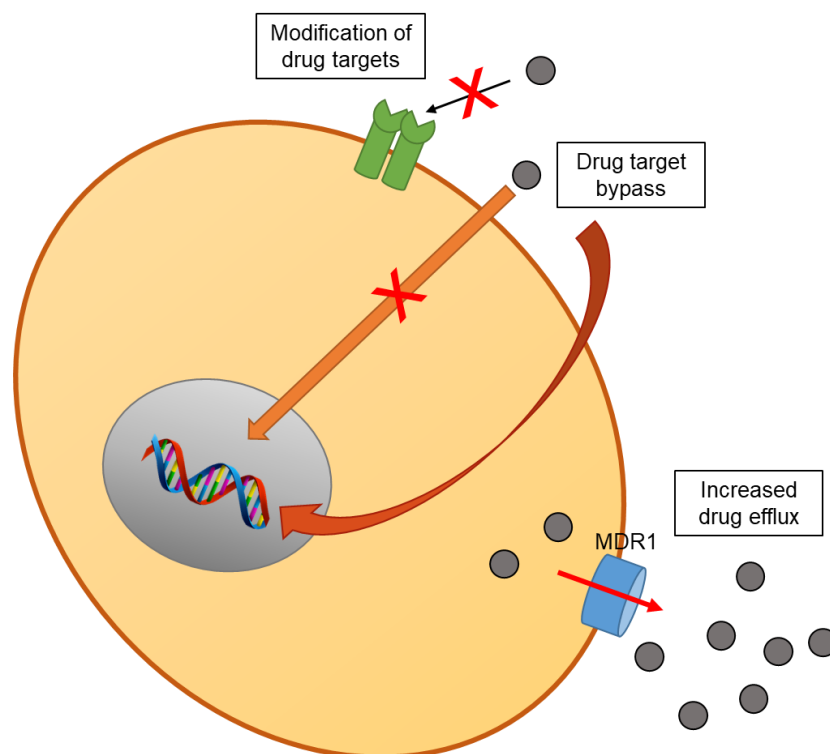


**Figure 4.3. Schematic diagram of three examples of drug resistance mechanisms.** Many drug resistance mechanisms have been identified; this diagram shows three simplified resistance mechanisms as described in section 1.X.X to 1.X.X.

#### 1.6.4. Resistance to PI3K/AKT pathway inhibitors

Despite this, there is still very little known about resistance to AKT inhibitors. One study has suggested that breast cancer cell lines with acquired resistance to the small-molecule allosteric AKT inhibitor MK-2206 have significantly elevated levels of Akt3. This is supported by evidence from siRNA knockdown of AKT3 which restores sensitivity to MK2206 in resistant cell lines, whereas knockdown of AKT1 or AKT2 has no effect on sensitivity (Stottrup, Tsang and Chin, 2016). However, further investigations into potential resistance mechanisms for these drugs remains an important issue in order to determine whether allosteric or ATP-competitive inhibition results in similar resistance mechanisms.

It has also been reported that some cell lines have intrinsic resistance to AKT inhibition, such as the E17K mutation in the lipid-binding PH domain of AKT. This results in decreased sensitivity to allosteric inhibition relative to wild-type AKT (Carpten *et al.*, 2007). Furthermore, investigation of the role of SGK1 in intrinsic resistance has also been carried out. SGK1 is a serine/threonine kinase which shares approximately 50% kinase domain homology with AKT, and is activated in a similar manner through phosphorylation by PDK1 and mTORC2. SGK1 also has the ability to regulate many of the same substrates as AKT such as GSK3 $\beta$  and FOXO3a (Kobayashi and Cohen, 1999; Brunet *et al.*, 2001), leading to

the hypothesis that SGK1 may override AKT activity in intrinsically resistant cell lines. Several breast cancer cell lines intrinsically resistant to inhibition by AZD5363 have been found to express high levels of SGK1, whereas AKT inhibitor-sensitive cell lines express low to undetectable SGK1 levels. Therefore, this suggests that SGK1 may be a driver of proliferation and survival in these resistant cells (Sommer *et al.*, 2013).

As more AKT inhibitors are being developed and entering preclinical and clinical studies, it is important to examine how acquired resistance mechanisms may arise in order to develop the most appropriate drug combinations for use in patients. Acquired resistance to novel molecular targeted drugs represents a significant barrier to the development of these drugs and their use in the clinic. Therefore, analysing resistance mechanisms to AKT inhibitors in breast cancer, a disease in which these drugs are currently being clinically evaluated, has the potential to affect therapeutic strategies to overcome this issue and directly impact patients.

### **1.7. Project aims and objectives**

Overall, deregulation of the PI3K/AKT is a key driver of breast cancer and the development of inhibitors of this pathway such as AZD5363 is promising for the future of cancer therapy. However, acquired resistance is a major obstacle to the efficacy of these kinds of targeted drugs. Acquired resistance has already been generated *in vitro* to CCT129254 (a precursor of AZD5363 (McHardy *et al.*, 2010)) in ovarian cancer models. Therefore, the aim of this project was to develop AZD5363-resistant breast cancer models and test the hypothesis that we will see the same resistance mechanism in both the ovarian and breast cancer models.

Objectives:

1. Characterise breast cancer cell lines sensitive to the experimental AKT inhibitor AZD5363
2. Generate AZD5363-resistant breast cancer cell line models
3. Quantify resistance in these breast cancer models
4. Investigate resistance mechanisms through examination of cross-resistance to other AKT inhibitors and changes in signalling
5. Develop a high-throughput cell-based ELISA method of investigating PI3K/AKT pathway signalling as an alternative to Western blotting

## **2.0 Materials and Methods**

### **2.1. Cell lines and culture**

Human breast cancer cell lines MCF-7 (American Type Culture Collection [ATCC]) and T47D (Sigma Aldrich) were grown in Dulbecco's Modified Eagle's medium (DMEM; Sigma Aldrich) supplemented with 10% foetal bovine serum (FBS; Sigma Aldrich). ZR-75-1 (Sigma Aldrich) was grown in RPMI-1640 medium (Sigma Aldrich) supplemented with 10% FBS. Cell lines were incubated in a humidified incubator at 37°C and 5% CO<sub>2</sub>. Cells were grown in T75 tissue culture flasks (Sarstedt), and passaging was performed when cell lines were approximately 70% confluent. Cells were passaged for no longer than three months to minimise phenotypic changes. During passage, cells were washed with phosphate-buffered saline (PBS) and detached with trypsin-EDTA (Sigma Aldrich). Cell lines were resuspended in the appropriate media (as previous) and split at an appropriate ratio (e.g. 1:10) to ensure logarithmic phase growth for experimental procedures.

### **2.2. Characterisation of cell line growth**

#### **2.2.1. Cell seeding density assays**

Cells were seeded in seven 96-well plates at cell densities varying from 800 cells/well to 12,800 cells/well in 200 µL of the appropriate culture media. After each 24-hour period, one plate was fixed with 70 µL 10% (w/v) trichloroacetic acid (TCA) and incubated at room temperature for 30 minutes, before being washed 5 times with distilled water and dried overnight at 37°C. 70 µL 0.4% Sulforhodamine B (SRB) in 1% acetic acid was added per well and incubated as above, then washed 5 times with 1% acetic acid. After drying overnight, plates were solubilised with 100 µL 10 mM Tris per well and placed on a shaker at 200 RPM for 10 minutes, and the OD read at 490 nm in a Victor X4 Multilabel Plate Reader (PerkinElmer Life Sciences).

#### **2.2.2. GI<sub>50</sub> determination**

GI<sub>50</sub> concentrations were determined by sulforhodamine B (SRB) growth assays. The GI<sub>50</sub> is defined as the concentration of drug required for half-maximal inhibition of cell growth. Cells were seeded in 96-well plates at the optimum seeding density for each cell line (section 2.1.X.). 40 µL of drug was added after 48 hrs incubation at concentrations from 10 µM to 0.08 µM AZD5363. 96 hrs after addition of drug, plates were fixed and stained as above, and the OD read at 490nm. GI<sub>50</sub> values were determined using GraphPad Prism 6 (GraphPad Software Inc.).

### 2.2.3. Propidium iodide staining and flow cytometry

T47D cells were exposed to either 0.1  $\mu\text{M}$  or 0.4  $\mu\text{M}$  AZD5363 for 48 hours in T75 tissue culture flasks. After 48 hours treatment, cells were trypsinised and centrifuged at 1200 RPM for 5 minutes. After aspiration of the supernatant, the pellet was resuspended in 5 mL PBS and centrifuged again as previous. The resulting pellet was suspended in 500  $\mu\text{L}$  PBS and fixed in ice-cold 70% ethanol whilst vortexing. Fixed cells were centrifuged as previous, and resuspended in 1 mL 20  $\mu\text{g}/\text{mL}$  propidium iodide and 50  $\mu\text{L}$  100  $\mu\text{g}/\text{mL}$  RNase A. Cells were then incubated for 30 minutes in the dark at room temperature. Cells were analysed using a FACSJazz™ (BD Biosciences) flow cytometer, recording 20,000 events at excitation wavelength 488 nm and measurement of red fluorescence at 542 nm.

### 2.3. Generation of AZD5363-resistant sub-clones

Clonal populations of MCF-7 and T47D human breast cancer cell lines were obtained through limiting dilution of cells in a 96-well format at a concentration of 0.5 cells per well. After 7 days, AZD5363 was added at concentrations of 2  $\mu\text{M}$  and 10  $\mu\text{M}$  to MCF-7 and T47D, and 0.1  $\mu\text{M}$ , 0.25  $\mu\text{M}$  and 0.5  $\mu\text{M}$  to ZR-75-1. Wells were monitored for the growth of clonal populations, and media with drug was replaced weekly. Once clones were approx. 50% confluent, cells were washed with sterile PBS and detached with trypsin, then transferred to a larger culture volume. The expansion process involved transfer from the

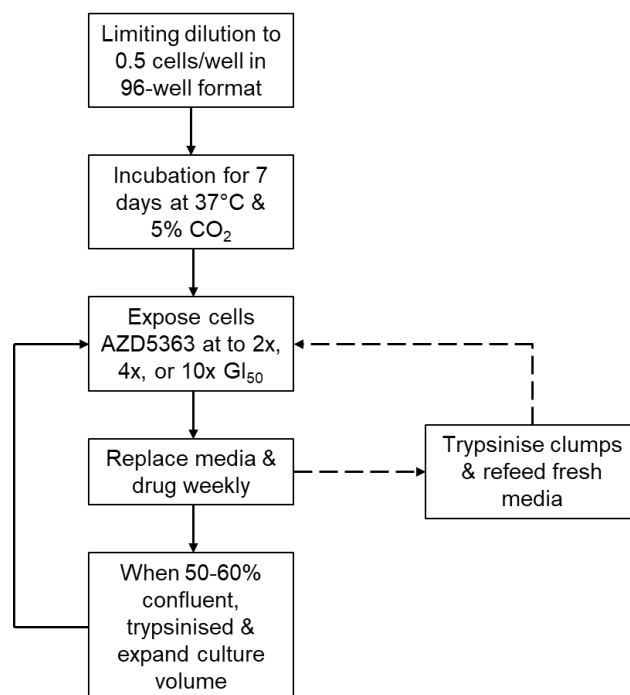


**Figure 2.1 – Flow diagram describing protocol of generating AZD5363-resistant clones.** Dotted lines indicate optional steps taken if cells form dense clumps (as with ZR-75-1), to prevent decreased growth due to contact inhibition.

96-well format to 24-well, then 6-well, until there were enough cells present for culture in T25 flasks.

## **2.4. Cell-based ELISA**

Cell lines were seeded in 96-well plates at a density of 16,000 cells per well, and allowed to attach overnight. Cells were then treated with concentrations of AZD5353 ranging from X  $\mu$ M to X  $\mu$ M and incubated for 1 hr at 37°C. Media was removed from all wells, and 100  $\mu$ L fixing solution (3% paraformaldehyde, 0.25% glutaraldehyde, 0.25% Triton X100) was added per well before incubating for 30 min at 37°C. Plates were washed 1x with water/0.1% Tween20, and blocked in 5% milk/tris-buffered saline with 1% Tween<sup>®</sup> 20 (TBST). Plates were washed as above and incubated overnight at 4°C with 100  $\mu$ L primary antibody (phospho- or total GSK3 $\beta$ /S6RP) diluted 1:250 in 5% milk/TBST. Plates were washed 3x as above, before being incubated for 1 hr at 37°C in 100  $\mu$ L of secondary antibody per well, diluted 1:1000 in 5% milk/TBST. Plates were washed 3x as above. 200  $\mu$ L o-phenylenediamine dihydrochloride (OPD) horseradish peroxidase (HRP) substrate (Sigma Life Science) was then added per well, and placed on a shaker for 15 minutes to allow an orange product to develop. The reaction was then stopped with the addition of 50  $\mu$ L 25% sulphuric acid. Optical density (OD) was determined using a Victor X4 Multilabel Plate Reader (PerkinElmer Life Sciences) at a wavelength of 490 nm.

## **2.5. Cell lysis and Western blotting**

### **2.5.1. Cell lysis**

Cell lines were plated in 10 cm dishes and allowed to adhere for 24-48 hours. T47D and MCF-7 were seeded at  $1 \times 10^5$  cells/mL, and both parental ZR-75-1 and resistant sub-clones were seeded at  $2 \times 10^5$  cells/mL. When plates were 60-70% confluent, media was aspirated from the dishes and washed twice with ice-cold PBS. 100  $\mu$ L ice-cold lysis buffer (50 mM HEPES pH 7.4, 250 mM NaCl, 0.1% Nonidet-P40, 1 mM DTT, 1 mM EDTA, 1 mM NAF, 10 mM  $\beta$ -glycerophosphate, 0.1 mM sodium orthovanadate, and Complete™ protease inhibitor cocktail [Roche, Switzerland]) was added to plates before being scraped. Lysates were transferred to ice-cold microcentrifuge tubes and incubated for 30 minutes. Lysates were centrifuged at 14,000 RPM for 10 minutes at 4°C to remove any insoluble material, and supernatants transferred to new microcentrifuge tubes. Tubes were kept on ice for immediate use, or snap-frozen in dry ice and stored at -80°C.

### **2.5.2. BCA protein determination assay**

Bovine serum albumin (BSA) standards were made at 0.1 mg/mL – 1.0 mg/mL to generate a standard curve. Lysates were diluted 1:20 in dd H<sub>2</sub>O, and 10  $\mu$ L of BSA standard and

lysate were plated in triplicate in a 96-well plate. 200  $\mu$ L of copper sulphate/bicinchoninic acid (BCA) solution (diluted 1:50) were added to each well and placed on a plate shaker for 1 minute. Plates were then incubated at 37°C for 1 hr, and read using a Victor X4 plate reader (Perkin Elmer) at 560 nm.

### 2.5.3. SDS-PAGE and Western blotting

Protein concentration of lysates were determined using the bicinchoninic acid (BCA) assay, and lysate concentrations were normalised in lysis buffer and 5X sample buffer. Samples were denatured by boiling at 95°C for 5 minutes, prior to loading on a 12% polyacrylamide gel for resolution at 150V for 60-90 minutes. Wet transfer was performed on a PVDF (polyvinylidene difluoride) membrane (Millipore) using a Mini Trans-Blot® cell apparatus (Bio-Rad) for 90 minutes at 100V. Correct protein transfer was examined through Ponceau S staining. The PVDF membrane was then blocked in 5% milk in TBST for one hour at room temperature, then incubated on a shaker overnight in primary antibody (see table 1 for antibodies used) and 5% milk/TBST at 4°C. Membranes were washed 2x for 10 minutes in TBST, then incubated in secondary antibody in 5% milk/TBST for one hour at room temperature. Membranes were washed again 4x for 5 minutes in TBST, then developed in ECL Western blotting substrate (Pierce) using a G:BOX Chemi XX6 (SynGene). Membranes were first probed using phospho-specific antibodies, then stripped and re-probed using total antibodies.

**Table 1. List of antibodies used for Western blot and ELISA analysis**

| Primary antibody          | Supplier        | Catalogue number | Species | Dilution |
|---------------------------|-----------------|------------------|---------|----------|
| AKT                       | Cell signalling | 4691             | Rabbit  | 1:1000   |
| AKT pS473                 | Cell signalling | 4060             | Rabbit  | 1:1000   |
| GSK3 $\beta$              | Cell signalling | 9832             | Mouse   | 1:1000   |
| GSK3 $\beta$ pS9          | Cell signalling | 5558             | Rabbit  | 1:1000   |
| 4EBP1                     | Cell signalling | 9644             | Rabbit  | 1:4000   |
| 4EBP1 pT37/T46            | Cell signalling | 2855             | Rabbit  | 1:1000   |
| ERK 1/2                   | Cell signalling | 4695             | Rabbit  | 1:1000   |
| ERK1/2 pT202/Y204         | Cell signalling | 4370             | Rabbit  | 1:1000   |
| p70 S6K                   | Cell signalling | 9202             | Rabbit  | 1:1000   |
| p70 S6K pT389             | Cell signalling | 9205             | Rabbit  | 1:500    |
| S6RP                      | Cell signalling | 2217             | Rabbit  | 1:4000   |
| S6RP pS235/236            | Cell signalling | 2211             | Rabbit  | 1:1000   |
| Tubulin alpha 1B          | Bio-Rad         | VPA00172         | Rabbit  | 1:1000   |
| Secondary antibody        | Supplier        | Catalogue number | Species | Dilution |
| Anti-mouse HRP conjugate  | Bio-Rad         | 170-6516         | Goat    | 1:10,000 |
| Anti-rabbit HRP conjugate | Bio-Rad         | 170-6515         | Goat    | 1:10,000 |

## 3.0 Results

### 3.1. Characterisation of parental cell lines

#### 3.1.1. Cell growth characteristics

Three human breast cancer cell lines were selected for this project; T47D, MCF-7 and ZR-75-1. These have been previously validated as sensitive to treatment with AZD5363, classified as having an  $GI_{50} < 3 \mu\text{mol/L}$ . (B. Davies *et al.*, 2012). There is significant correlation between sensitivity to AZD5363 and the presence of activating mutations in *PIK3CA* or mutations resulting in loss of *PTEN*; additionally, cell lines positive for overexpression of HER2 and/or ER are consistently sensitive to the drug. Therefore, the cell lines selected for analysis reflect these properties, and are summarised in table 2. In addition to having activating mutations in *PIK3CA*, T47D and MCF-7 have also have increased *PIK3CA* gene copy number, with over four copies per cell.

**Table 2. Human cancer cell lines used and associated PI3K/AKT pathway aberrations.** Receptor expression status indicates the presence or absence of oestrogen receptor (ER), progesterone receptor (PR), and human epidermal growth factor (HER2) expression.

| Cell line | Disease type          | PI3K/AKT pathway aberration  | Receptor expression status |
|-----------|-----------------------|--|----------------------------|
| MCF-7     | Breast adenocarcinoma | PIK3CA E545K (exon 9) substitution in helical domain; high GCN <sup>1</sup>    | ER+ PR+ HER2-              |
| T47D      | Ductal carcinoma      | PIK3CA H1047R (exon 20) substitution in kinase domain; high GCN <sup>1,2</sup> | ER+ PR+ HER2-              |
| ZR-75-1   | Ductal carcinoma      | PTEN L108R substitution and weak expression <sup>3</sup>                       | ER+ PR+ HER2+              |

<sup>1</sup> G. Wu *et al.* 2005, <sup>2</sup> L.H. Saal *et al.* 2005, <sup>3</sup> B. Weigelt *et al.* 2011

Light microscopy images were obtained to examine the morphology of the parental cell lines, as seen in figure X. For example, ZR-75-1 cells are semi-adherent and attach only very lightly to the culture vessel. Additionally, it is not abnormal for this cell line to not form a confluent monolayer, readily forming large piled clusters of cells growing in many layers. On the other hand, T47D and MCF-7 form smooth monolayers with tight cohesive structures and strong cell-cell adhesions (Figure 3.1).

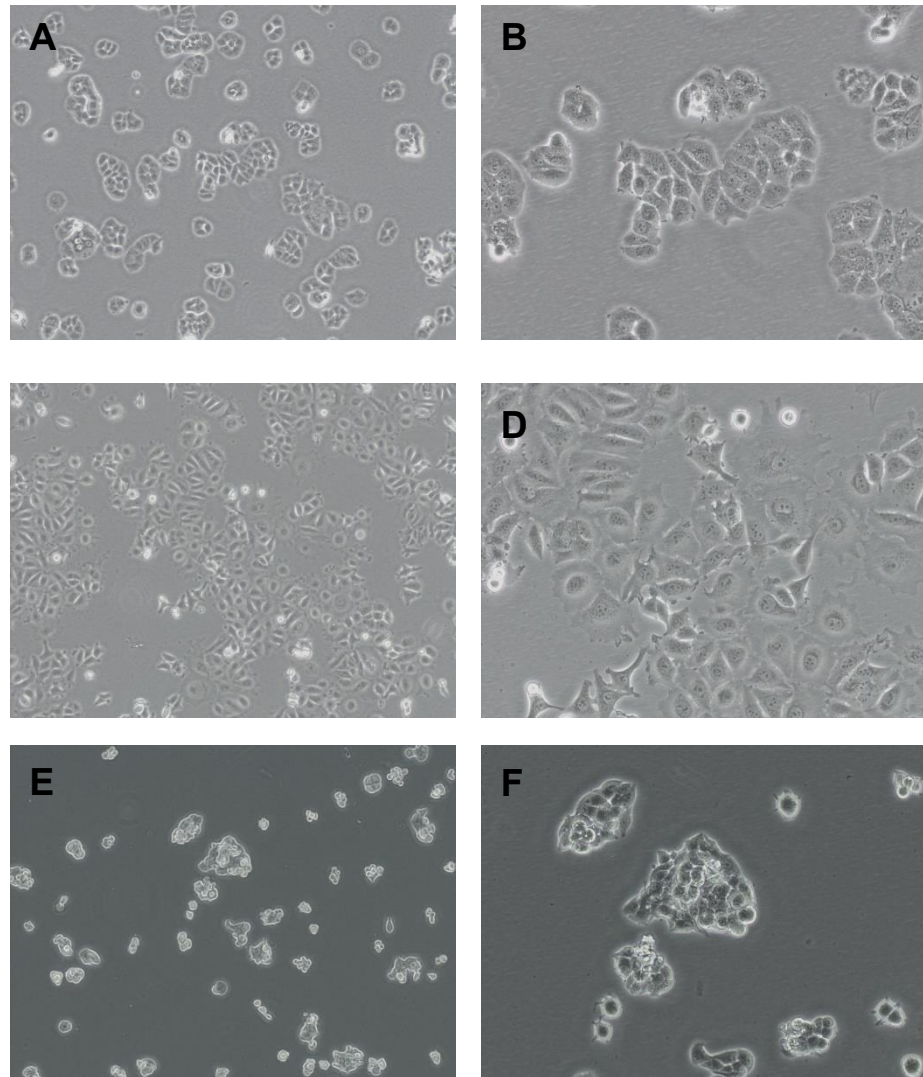
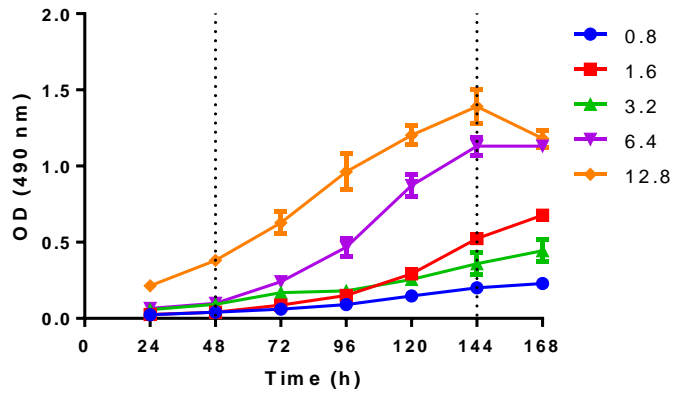


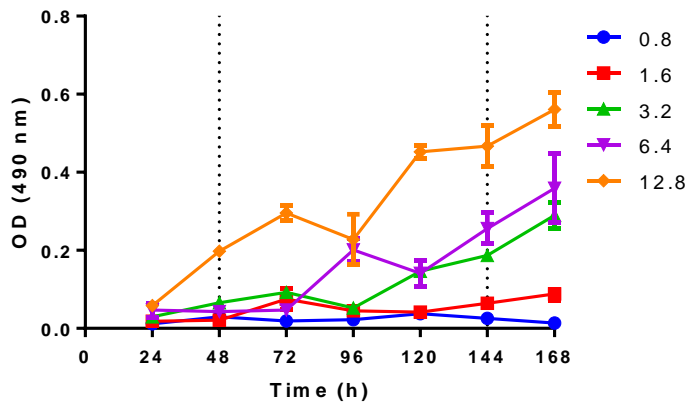
**Figure 3.1. Brightfield microscopy images of breast cancer cell lines in culture.** Images of T47D, MCF-7, and ZR-75-1 at x40 magnification (A, C & E) and x100 magnification (B, D & F). Images taken using Olympus CKX53 microscope.

Sulforhodamine B (SRB) assays were to be carried out to determine the half-maximal growth inhibitory concentration ( $GI_{50}$ ) of AZD5363 in these cell lines. However, in order to undertake this, seeding density assays were performed. This was to determine the optimal concentration of cells to be seeded per well in a 96-well format to ensure logarithmic phase growth for the duration of the 96-hour SRB assay, taking into account the doubling times of individual cell lines. This ensures that any changes in cell viability are due to the action of the drug, and not due to growth arrest from over-confluent cells undergoing contact inhibition. To carry out these seeding density assays, seven 96-well plates were seeded for each cell line at five different cell densities. One plate was fixed every 24 hours, and stained with SRB, a purple dye that binds to negatively charged amino acids. When excess SRB was washed out and the bound dye solubilised in tris, the intensity of the staining can be monitored colourimetrically in the plate reader to obtain a measure of cell viability. The subsequent growth curves were examined, the seeding densities that permitted log phase growth between 48 and 144 hours (the duration of the assay) were selected. Therefore, densities of 6,400 cells per well were selected for cell lines MCF-7 and T47D, and 12,800 cells per well for ZR-75-1 (fig X).

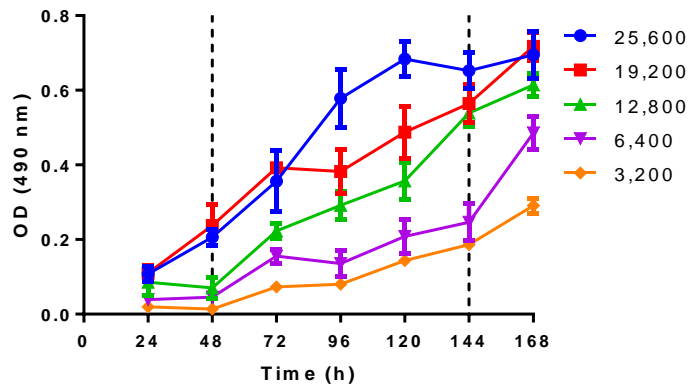
MCF-7 optimum seeding density



T47D



ZR-75-1 optimum seeding density assay



### **3.1.2. GI<sub>50</sub> determinations for T47D, MCF-7 and ZR-75-1 cell lines**

Using the selected seeding densities, SRB assays were performed to determine the GI<sub>50</sub> of AZD5363 for each cell line. Cells were seeded at their optimum density for the 96-hour assay, and were treated with a range of concentrations of AZD5363 48 hours after seeding. 96 hours post-treatment, plates were fixed and stained to generate cell viability curves (Figure 3.2). A summary of the GI<sub>50</sub> values generated can be found in table X. This reveals that MCF-7 is the least sensitive to AZD5363, with a GI<sub>50</sub> of 1.34 µM. This is followed by T47D with a GI<sub>50</sub> of 0.92 µM, with ZR-75-1 the most sensitive at 0.05 µM. This pattern of sensitivity between these three cell lines seen here is notable as it follows the same trend as seen in previous preclinical studies (B.R. Davies, 2012).

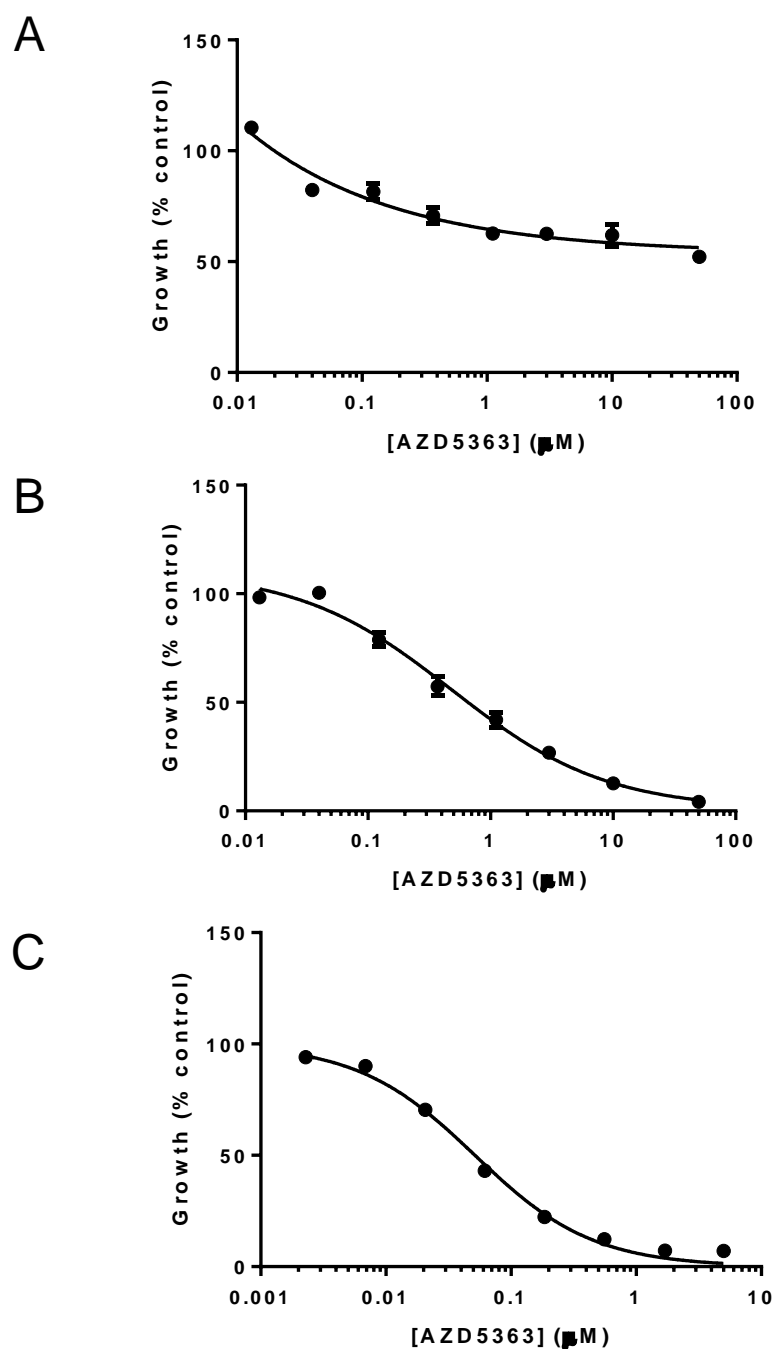
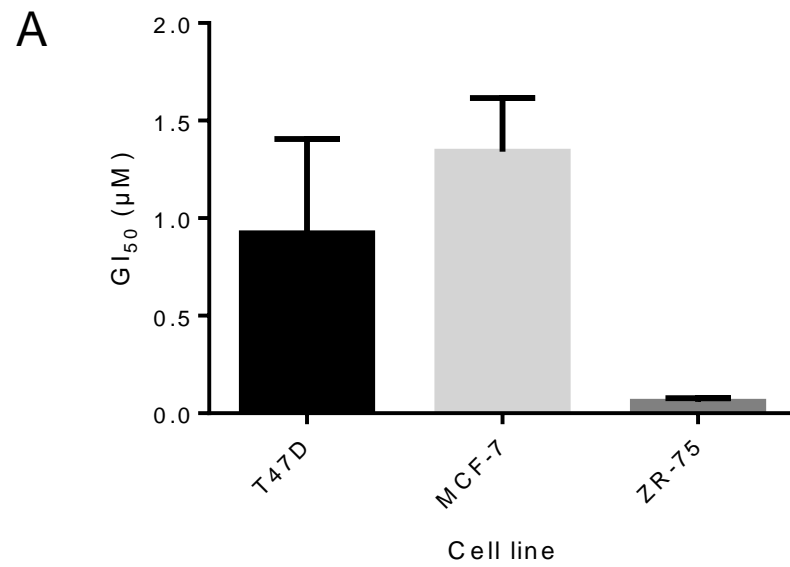


**Figure 3.3. Cell viability curves of breast cancer cell lines treated with AZD5363, determined by SRB assay as a percentage of untreated controls.** Growth curves were obtained for cell lines (A) T47D, (B) MCF-7 and (C) ZR-75-1. A summary of GI<sub>50</sub> values can be found in figure X.X. Data are representative of n = 3 independent experiments. Data points represent mean ± standard deviation.



**B**

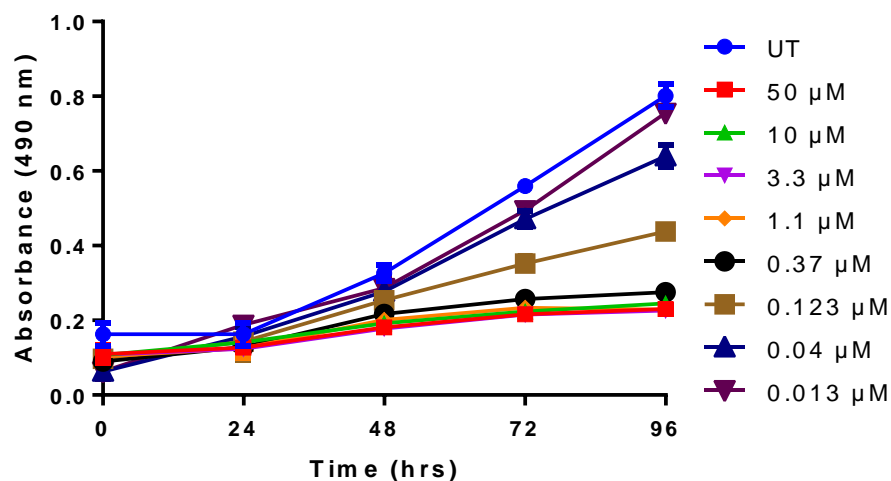
| Cell line | AZD5363<br>GI <sub>50</sub> ± SD (µM) |
|-----------|---------------------------------------|
| T47D      | 0.92 ± 0.39                           |
| MCF-7     | 1.34 ± 0.22                           |
| ZR-75-1   | 0.05 ± 0.01                           |

**Figure 3.4. Summary of GI<sub>50</sub> values for AZD5363 in human breast cancer cell lines T47D, MCF-7 and ZR-75-1.** Bars in graph A and values in table B represent mean ± standard deviation.

Despite these data fitting trends in the literature, it can be seen from figure 3.3 that T47D did not have the same response as MCF-7 and ZR-75-1 after AZD5363 treatment. This is because both MCF-7 and ZR-75-1 reached close to 0% viability when treated with high concentrations of the drug. In contrast, cell viability for T47D remains at approximately 50% despite treatment with up to 50  $\mu\text{M}$  AZD5363. This effect was examined further to determine if these drug concentrations do indeed kill 50% of the cells, or if instead the growth of these cells was arrested after addition of the drug, as this would give the impression that 50% had survived relative to the untreated cells. To achieve this, a modified SRB assay was performed to analyse the effect of drug treatment on T47D over time. Five 96-well plates were seeded, four were treated with AZD5363 after 48 hours and one untreated plate was fixed to give 'zero hours' of treatment. These plates were analysed by SRB assay and plotted in figure 3.5. These data show that treatment of T47D with AZD5363 from 0.013  $\mu\text{M}$  to 0.37  $\mu\text{M}$  slows doubling time in a dose-dependent manner. The equation used to calculate doubling time is shown below, and a summary of T47D doubling times when exposed to various concentrations of AZD5363 can be found in figure 3.5.

$$\text{Doubling time} = \frac{\text{Duration} * \log(2)}{\log(\text{Final Concentration}) - \log(\text{Initial Concentration})}$$

However, when treated with more than 0.37  $\mu\text{M}$  cell growth is arrested, with concentrations up to 50  $\mu\text{M}$  all yielding the same effect on cell growth. This is because the absorbance of cells at the end of the 96-hour period treated with 50  $\mu\text{M}$  is not significantly higher than that of the untreated cells at the start of the assay. Taken together, this suggests that AZD5363 has more of an cytostatic effect on T47D, whilst treatment of MCF-7 and ZR-75-1 with this drug has more of a cytotoxic effect on these cells.



| AZD5363 concentration (μM) | Doubling time (hours) |
|----------------------------|-----------------------|
| 0.013                      | 26.79                 |
| 0.040                      | 28.64                 |
| 0.123                      | 44.16                 |
| 0.370                      | 59.31                 |
| 1.100                      | 83.10                 |
| 3.300                      | 89.74                 |
| 10.00                      | 80.49                 |
| 50.00                      | 89.48                 |

**Figure 3.5. Investigation of growth of T47D cells when treated with a range of concentrations of AZD5363 over time.** SRB assay plates were fixed every 24 hours after drug exposure to analyse the response of T47D to AZD5363 over the period of the 96-hour SRB assay. UT = untreated control. Data are representative of  $n = 2$  independent experiments, and data points represent mean  $\pm$  standard deviation.

The induction of growth arrest was further investigated through propidium iodide staining and flow cytometry to determine the phase of the cell cycle in which growth arrest occurs. T47D cells were treated with approximately 1x and 4x the  $GI_{50}$  of AZD5363 (0.1  $\mu$ M and 0.4  $\mu$ M) for 48 hours, then fixed and stained with propidium iodide (PI). This allows determination of the percentage of cells in each stage of the cell cycle as PI is a nucleic acid stain, and intensity of fluorescence detected by the flow cytometer is proportional to the DNA content of each cell. Therefore, cells in G<sub>2</sub>/M phase with 4N DNA will fluoresce twice as brightly as those in G<sub>0</sub>/G<sub>1</sub> phase with 2N DNA. The resulting histogram for untreated T47D cells shown in figure 3.6.A is similar to previously reported profiles (Kampa *et al.*, 2004). However, the profiles of T47D cells treated with either 0.1  $\mu$ M or 0.4  $\mu$ M in figures 3.6.B and 3.6.C respectively are not significantly different from that of the untreated. This suggests that cell cycle arrest has not been induced at a specific cell cycle transition. However, due to dose-dependent decreases in cell growth previously seen in figure 3.5 this may suggest that cell growth is arrested in all phases. This therefore requires further investigation.

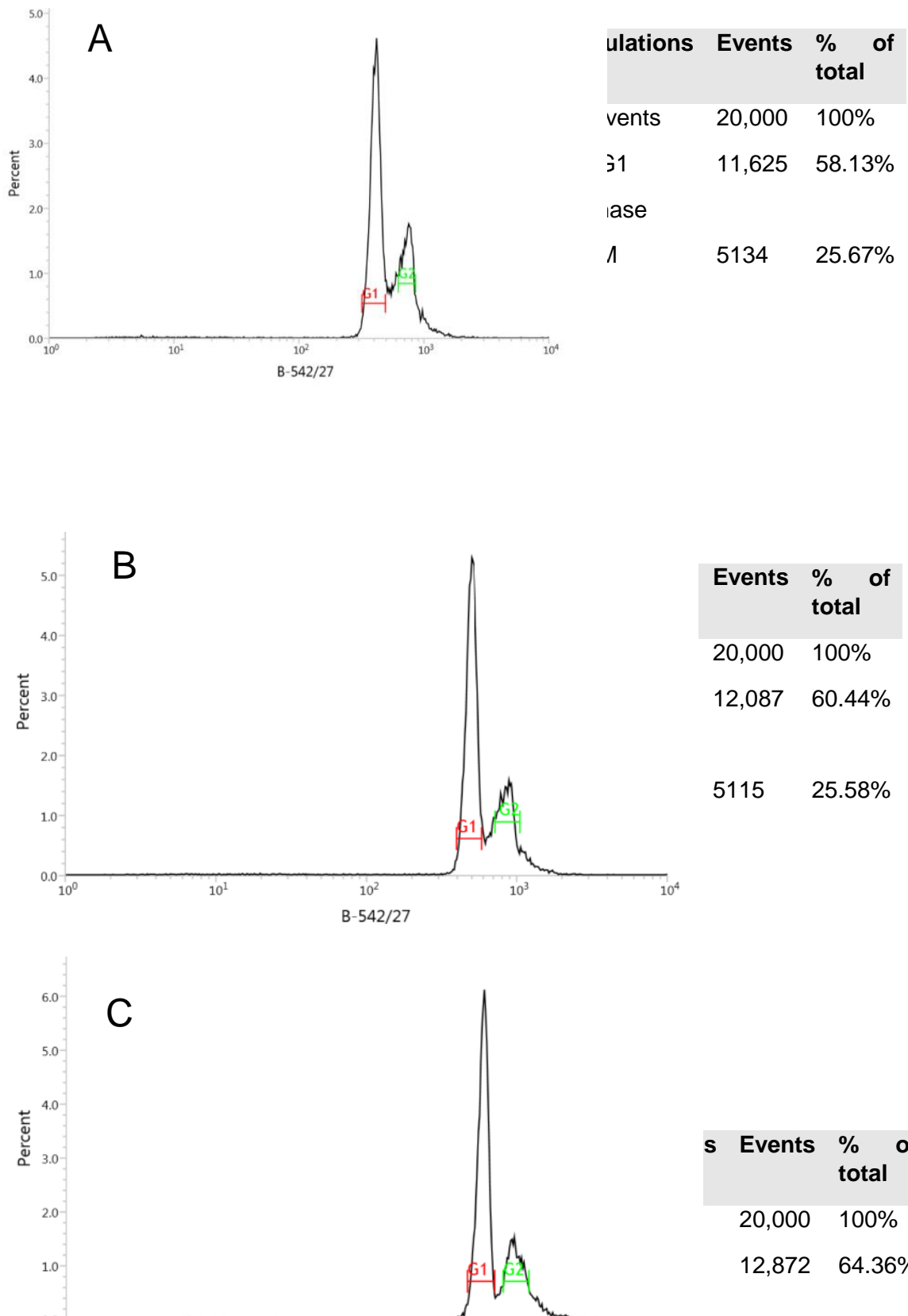


**Figure 3.6. Cell cycle analysis of T47D treated with AZD5363.** Cells were either untreated (A) or exposed to either 0.1  $\mu$ M (B) or 0.4  $\mu$ M (C) for 48 hours. Cells were then fixed and stained with propidium iodide and their fluorescence detected by flow cytometry. Results are representative of n=1 independent experiment. Y axis represents percentage of 20,000 recorded events, X axis represents fluorescence intensity at 542 nm.

### 3.1.3. Baseline signalling of parental cell lines

Western blotting was carried out to investigate PI3K/AKT signalling in the parental T47D, MCF-7 and ZR-75-1 cell lines. Phosphorylated and total AKT levels were investigated, along with selected proteins downstream of AKT on the pathway such as GSK3 $\beta$  (which is directly phosphorylated by AKT), 4EBP1, S6K, and S6RP. ERK was included as an indicator of MAPK pathway signalling (see Figure 1.1).

Lysates of untreated cells were used for analysis of basal signalling. Across the three cell lines, the levels of both total AKT (t-AKT) and AKT phosphorylated at serine 473 (pS473 AKT) remain consistent. Total GSK3 $\beta$  is also consistent, however phosphorylation appears to be higher in T47D and ZR-75-1 compared to MCF-7. For 4EBP1, levels of phosphorylation were low in T47D and MCF-7 relative to ZR-75-1 which was notably higher. Additionally, MCF-7 appears to have much higher levels of S6RP compared to T47D and ZR-75-1. Although not a member of the PI3K/AKT pathway, ERK signalling was investigated to the abundance in cross-talk between these pathways. This revealed that there was little phosphorylated ERK present in ZR-75-1, whereas levels of total and phosphorylated ERK remain consistent across T47D and MCF-7. Tubulin was included as a loading control, and levels are consistent across all three cell lines as the same protein concentration was loaded for all samples.

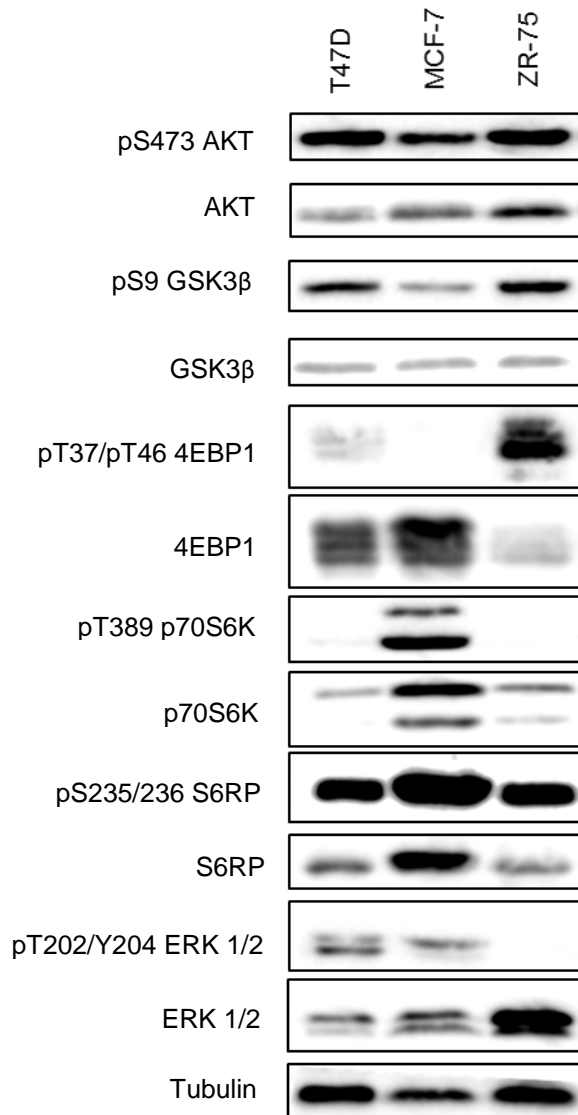


**Figure 3.7. Western blotting of parental cell lines to assess baseline signalling.** Western blotting protocol was used as described in section X.X. to investigate presence of various components of the PI3K/AKT pathway. Blots were probed using phospho-specific antibodies, then stripped and re-probed for the total signal. Tubulin was used as a loading control. Results are representative of n=2 independent experiments.

### 3.2. Generation and characterisation of AZD5363-resistant clones

Resistant clones were generated as in materials and methods section X.X. Parental cells underwent limiting dilution to be plated at 0.5 cells per well in a 96-well format. This was to reduce the probability of not obtaining clonal populations by preventing plating more than one cell per well. After incubation for one week to allow for adherence and several cell divisions, AZD5363 was added at concentrations of 2x, 4x and 10x the  $GI_{50}$ . Fresh media and drug was added weekly to ensure adequate supply of nutrients and continual exposure to the drug. After several weeks of culturing clonal populations of cells in 96-well plates, cells reached 50% confluency and were trypsinised and transferred to 24-well plates. This process was repeated for transfer into 6-well plates and T25 tissue culture flasks as the cell populations grew, as described in figure 2.1. Two clones from the ZR-75-1 cell line that had been cultured in 2x the  $GI_{50}$  (0.1  $\mu$ M AZD5363) were successfully expanded into tissue culture flasks as seen in figure 3.8. The two ZR-75-1 clones were named B9 and D2 for their location in the 96-well format. Small populations cultured in 4x and 10x eventually underwent growth arrest and were therefore not taken forward. Additionally, T47D and MCF-7 cells also did not continue to grow in any AZD5363 concentration once transferred to 24-well plates, and were also not taken forward.

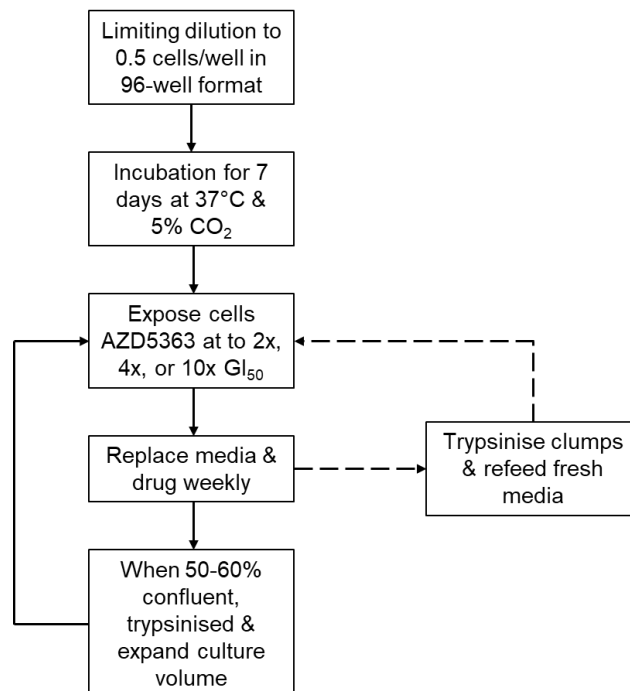
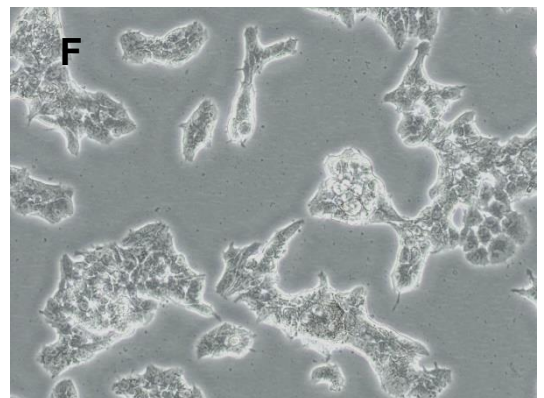
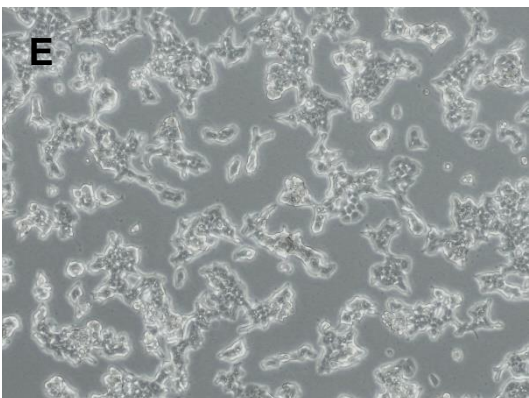
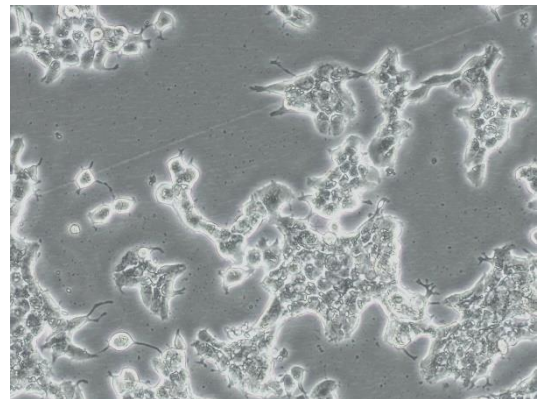
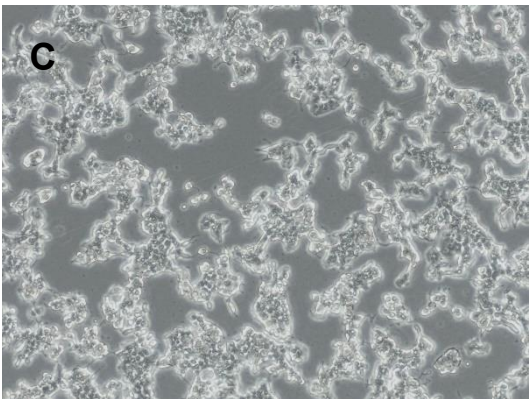
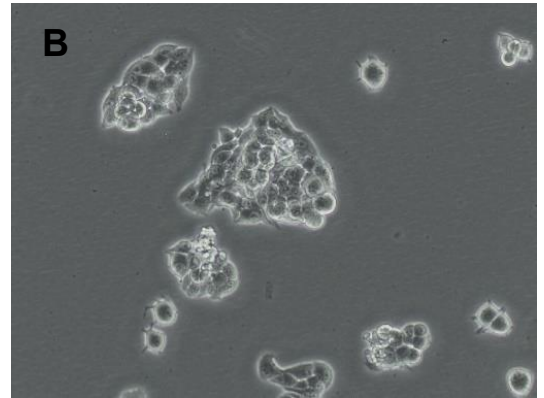
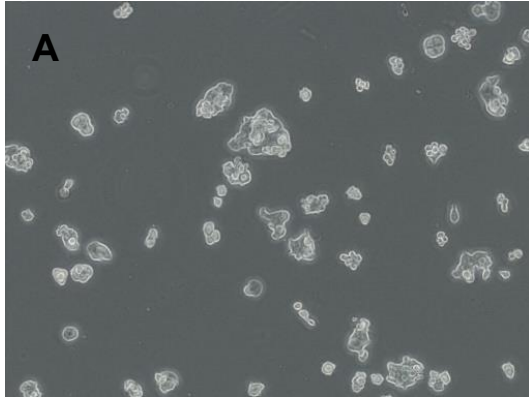


**Figure 2.1. Flow diagram describing protocol of generating AZD5363-resistant clones.** Dotted lines indicate optional steps taken if cells form dense clumps (as with ZR-75-1), to prevent decreased growth due to contact inhibition.

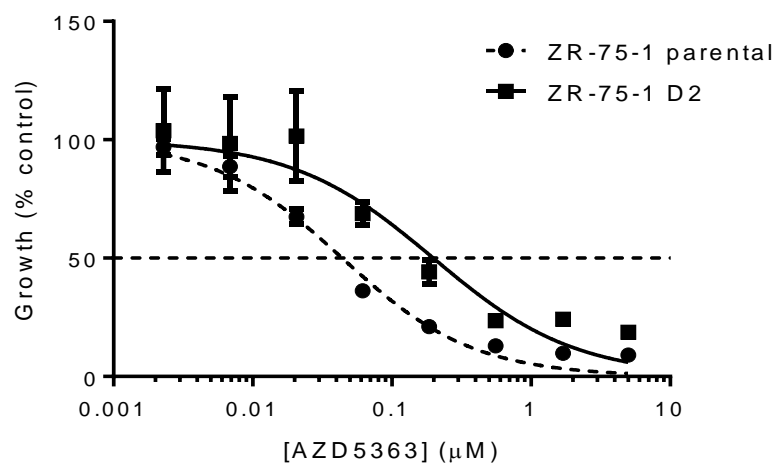
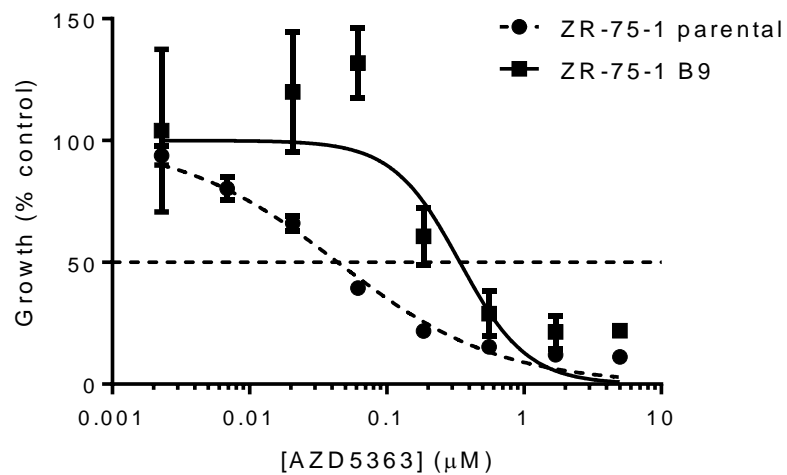


### 3.2.1. Determination of resistance factor in sub-clones

The ZR-75-1 sub-clones B9 and D2 were then investigated by SRB assay to determine the  $GI_{50}$  of AZD5363 in these newly-generated cells. The  $GI_{50}$  values obtained were then used to quantify the level of observed resistance. The ratio of resistant to parental  $GI_{50}$  was calculated to give the resistance factor i.e. the fold-resistance relative to the parental.

$$\text{Resistance factor (RF)} = \frac{\text{Resistant } GI_{50}}{\text{Parental } GI_{50}}$$

The growth curves obtained are shown in figure 3.9. The shift of growth curves to the right shows resistance was generated; clones B9 and D2 were shown to have resistance factors of 7.3 and 5.8-fold, respectively.

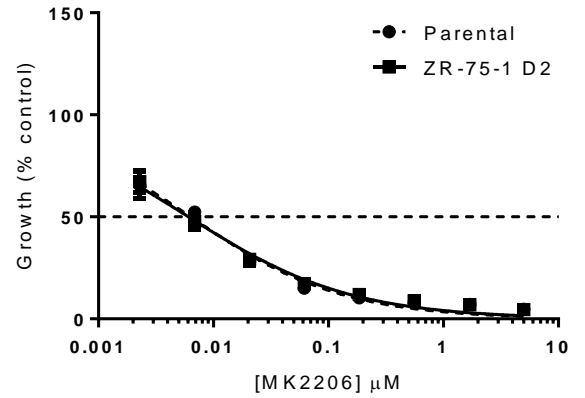
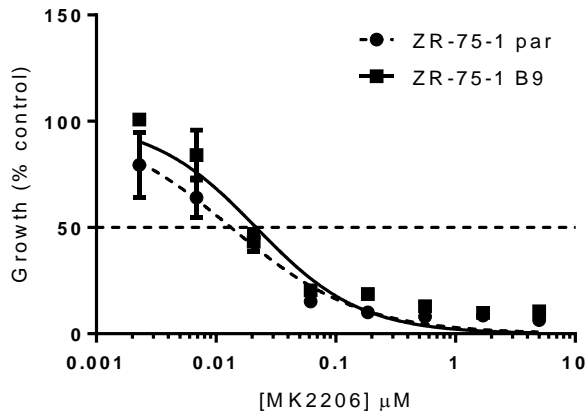


### **3.2.2. Determination of AKT inhibitor cross-resistance in sub-clones**

To investigate cross-resistance to other AKT inhibitors AZD5363-resistant sub-clones were treated with two other experimental AKT inhibitors, GDC0068 and MK-2206, which are currently under evaluation in clinical trials. GDC0068 shares the same mechanism of action as AZD5363 in that they are both ATP-competitive, whilst MK-2206 functions allosterically. Sensitivity was investigated via SRB assay, and cells were treated with a range of concentrations of each drug. Dose-response curves were generated (Figure 3.10) for parental ZR-75-1 as well as clones B9 and D2, with both GDC0068 and MK-2206.

These assays revealed that parental ZR-75-1 is also sensitive to inhibition by both GDC0068 and MK-2206. GDC0068 had a  $GI_{50}$  in the parental of 0.114  $\mu$ M, whereas these cells were notably more sensitive to inhibition by MK-2206 with a  $GI_{50}$  of 0.011  $\mu$ M. Interestingly, the AZD5363-resistant sub-clones showed no significant cross-resistance to either GDC0068 or MK-2206 (figure 3.11).

A



B

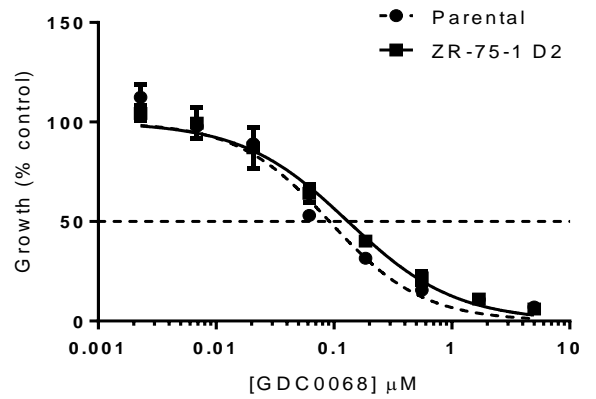
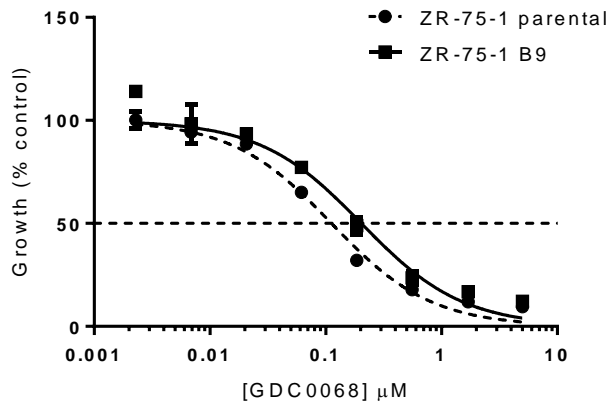
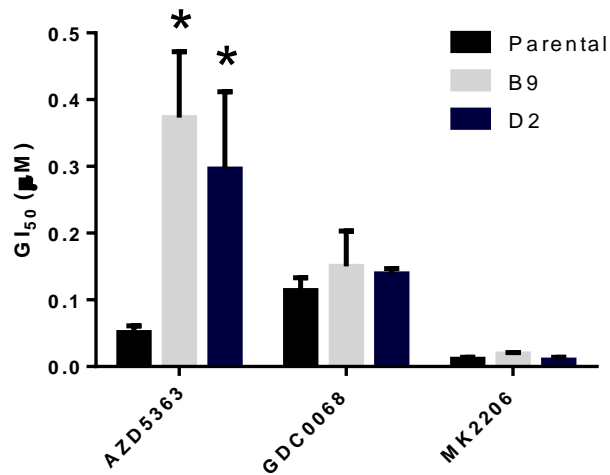


**Figure 3.10. SRB assays of resistant clones treated with A) MK-2206 and B) GDC0068.** Resistant clones B9 and D2 were treated with different concentrations of GDC0068 and MK-2206 to generate dose-response curves and GI<sub>50</sub> values (summarised in table). Data are representative of n = 3 independent experiments, and data points represent mean ± SD. Table gives IC<sub>50</sub> values represented as mean ± SD, and resistance factor (RF) as the ratio of resistant GI<sub>50</sub> to parental GI<sub>50</sub>.



| Drug          | Target                | GI <sub>50</sub> (µM) |               |               | Resistance Factor |        |
|---------------|-----------------------|-----------------------|---------------|---------------|-------------------|--------|
|               |                       | Parental              | B9            | D2            | B9                | D2     |
| AZD5363 (µM)  | AKT (ATP-competitive) | 0.051 ± 0.01          | 0.373 ± 0.099 | 0.296 ± 0.116 | 7.32 *            | 5.82 * |
| GDC-0068 (µM) | AKT (ATP-competitive) | 0.114 ± 0.019         | 0.150 ± 0.053 | 0.139 ± 0.008 | 1.31              | 1.22   |
| MK-2206 (µM)  | AKT (allosteric)      | 0.011 ± 0.003         | 0.019 ± 0.002 | 0.010 ± 0.004 | 1.83              | 0.97   |

**Figure 3.11. GI<sub>50</sub> values for AKT inhibitors in the ZR-75-1 parental and resistant clones B9 and D2.** Summary graph (A) and table (B) of GI<sub>50</sub> values for AKT inhibitors tested and resistance factor obtained. Data represent n = 3 independent experiments. Student's t-test \* p < 0.05.

### 3.2.3. Baseline signalling in resistant sub-clones

As AZD5363 acts to inhibit AKT, the main signalling node of the PI3K/AKT pathway, it was therefore important to examine the markers of AKT pathway signalling in the resistant sub-clones. Figure 3.12 shows analysis of AKT pathway components by Western blot in the parental line and resistant sub-clones with no drug treatment i.e. baseline signalling. Notably, this shows that there was no significant difference in PI3K/AKT signalling between the parental ZR-75-1 and sub-clones B9 and D2. For example, both AKT and GSK3 $\beta$  signalling remains consistent across the three cell types. Additionally, S6RP signalling downstream of mTORC1 is maintained from the parental to the sub-clones as levels of phosphorylated and total S6RP also remains consistent.

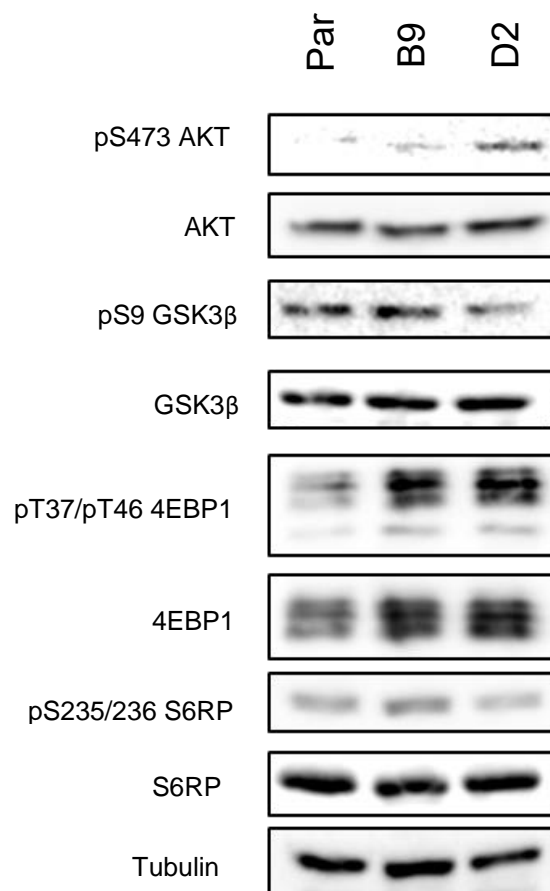
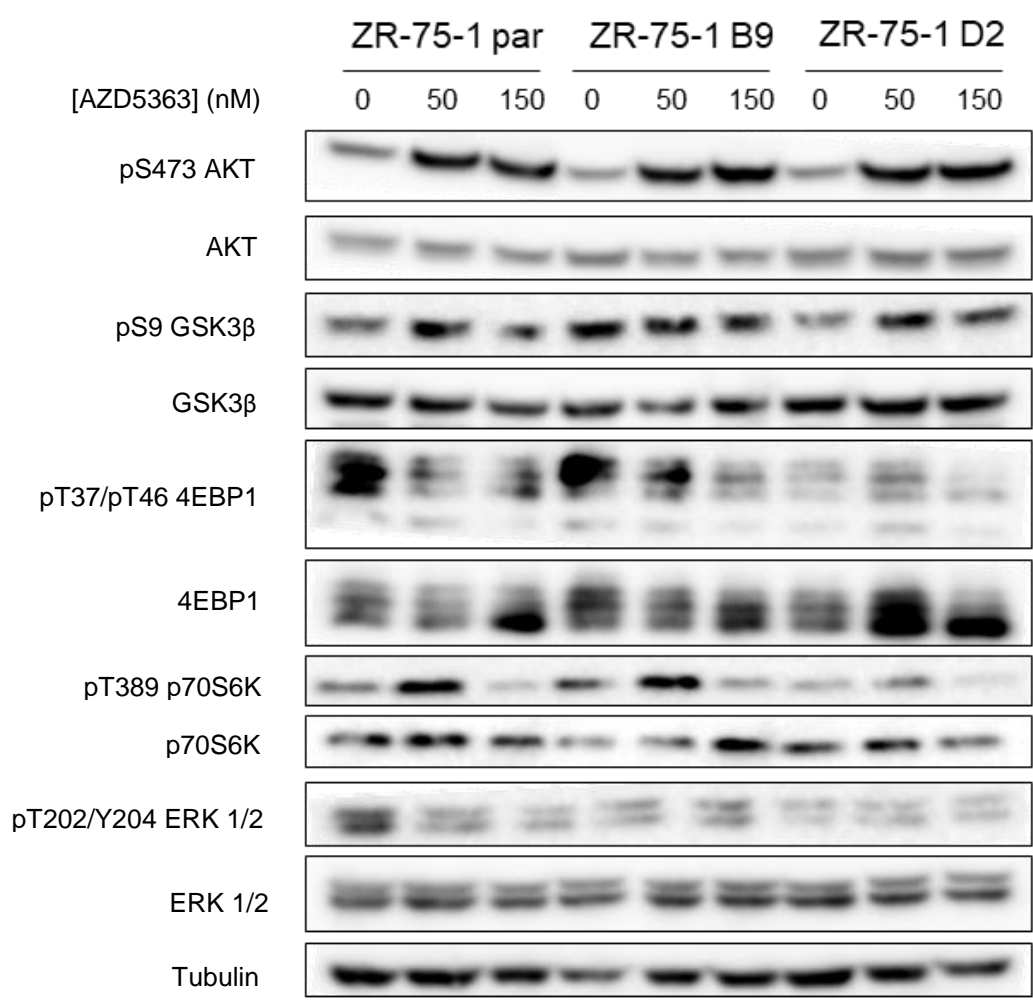


**Figure 3.12. Western blotting of untreated parental ZR-75-1 cell lines and AZD5363-resistant sub-clones B9 and D2 to assess baseline signalling.** Western blotting protocol was used to investigate PI3K/AKT pathway signalling. Blots were probed using phospho-specific antibodies as shown above, then stripped and re-probed for the total signal. Tubulin was used as a loading control. Par = parental ZR-75-1. Results are representative of n=2 independent experiments.

### 3.2.4. Response of resistant sub-clones to AZD5363

PI3K/AKT signalling of the resistant sub-clones versus the parental ZR-75-1 cell line in response to AZD5363 exposure was initially investigated through Western blotting. Cells were either untreated or treated with 50 nM or 150 nM of AZD5363 (1x and 3x parental GI<sub>50</sub>, respectively) for four hours before being lysed and separated via SDS-PAGE and subsequently transferred to a polyvinylidene fluoride (PVDF) membrane and probed with antibodies specific to the selected targets.

Results of this dose-response blot in Figure 3.13 show increased AKT serine 473 phosphorylation upon AZD5363 – a well described phenomenon in response to ATP-competitive inhibitors, caused by hyperphosphorylation of the protein as a result of conformational changes induced by occupation of the ATP binding pocket (Chan *et al.*, 2011). However, there is no significant change in the phosphorylation of GSK3 $\beta$  (a direct substrate of AKT) for sub-clones B9 and D2 or in the parental. Phosphorylation of 4EBP1 decreased with increasing drug concentration in both ZR-75-1 parental and B9, whereas phospho-4EBP1 levels in D2 remained low throughout. Decreased phospho-4EBP1 signal was also associated with shifting down of total 4EBP1 bands due to the lack of phosphate groups and the subsequent decrease in molecular weight. Furthermore, there was no significant difference in phosphorylation of S6K in the parental or the sub-clones in response to treatment with AZD5363.



### 3.1.5. Optimisation of cell-based ELISA

The possibility of using a cell-based ELISA as an alternative to Western blotting investigated. This technique can be likened to immunohistochemistry (IHC) in a 96-well format with respect to analysis of proteins in tissues, but generating quantitative data instead of visualisation. This therefore allows for statistical analysis, in contrast to the qualitative data generated from Western blots and IHC staining. The baseline signalling of the untreated parental ZR-75-1 cell line was first investigated for its GSK3 $\beta$  (Figure 3.14) and S6RP (Figure 3.15) signalling. This was to establish assays for targets directly downstream of both mTOR and AKT, respectively. Antibodies for both total and phosphorylated proteins were used to assess the activation one step down the pathway (GSK3 $\beta$ ) as well as further downstream (S6RP). Furthermore, two different ELISA substrates were investigated; a time-resolved fluorometric Europium substrate and a colourimetric *o*-phenylenediamine dihydrochloride (OPD) substrate to detect horseradish peroxidase (HRP). Similar assays have been developed for targets such as retinoblastoma protein (pRb) but this is a novel method for detection of S6RP phosphorylation (Barrie *et al.*, 2003). A matrix of various concentrations of primary and secondary antibodies was used in order to determine the optimal antibody concentrations for each assay.

The Europium chelate immunoassay resulted in significantly higher signal-to-noise ratios in comparison to the OPD substrate. For example, a 1:250 pGSK3 $\beta$  antibody dilution yields a signal-to-noise ratio of 6.3 for the Europium chelate and 1.8 for OPD. This is thought to be because the Europium chelate assay uses time-resolved fluorescence, whereby there is a relatively long fluorescence decay time and large Stokes' shift (difference in excitation and emission wavelengths). This therefore reduces the influence of any background autofluorescence.

From these optimisation assays, the Europium chelate substrate was selected for further use due to the increased signal-to-noise ratio. Additionally, the primary antibody concentrations selected (for both total and phospho-specific antibodies) were 1:1000 for S6RP and 1:250 for GSK3 $\beta$ . A concentration of 1:3333 (as recommended by the manufacturer) was selected for the anti-rabbit Europium chelate secondary antibody.

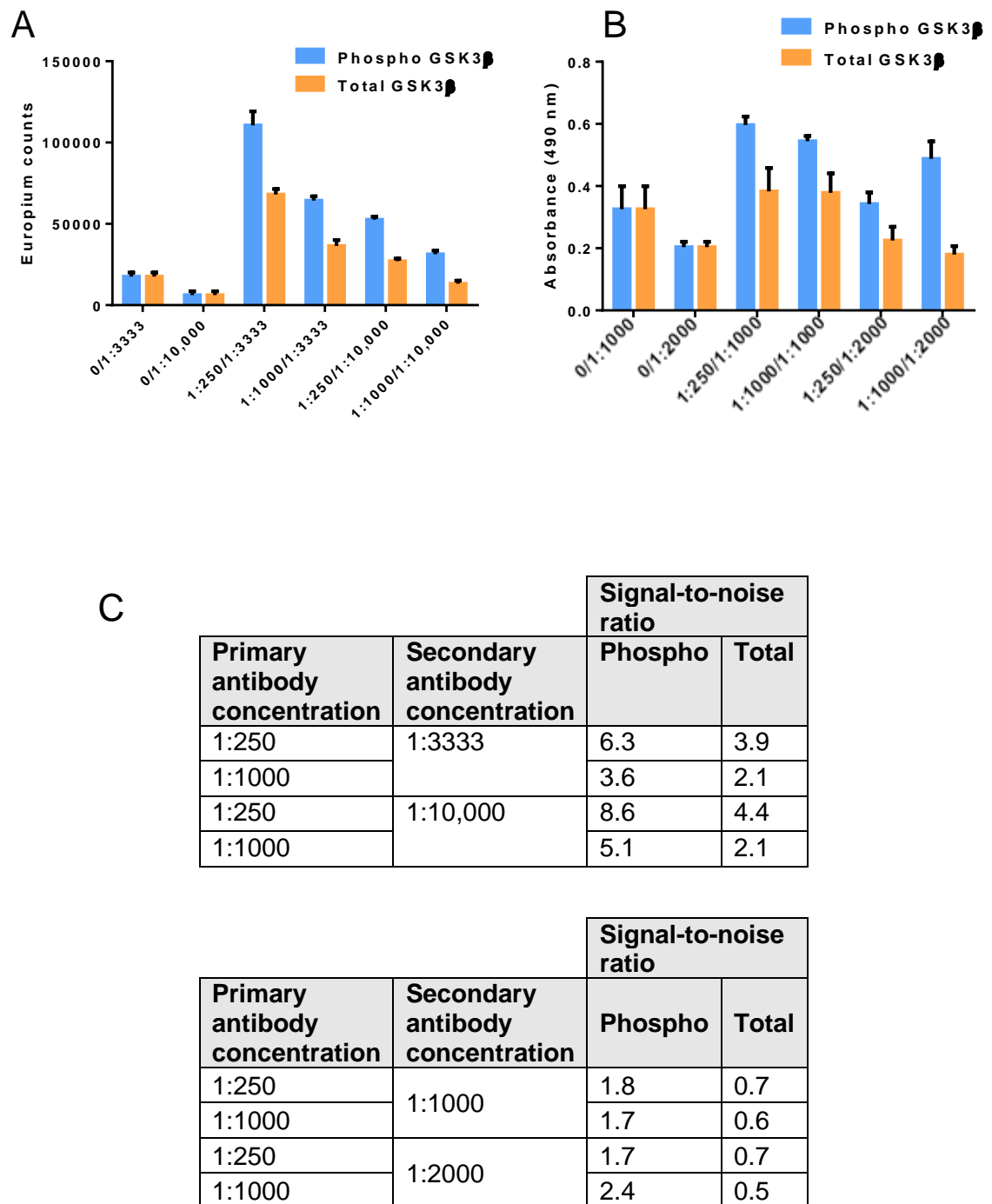
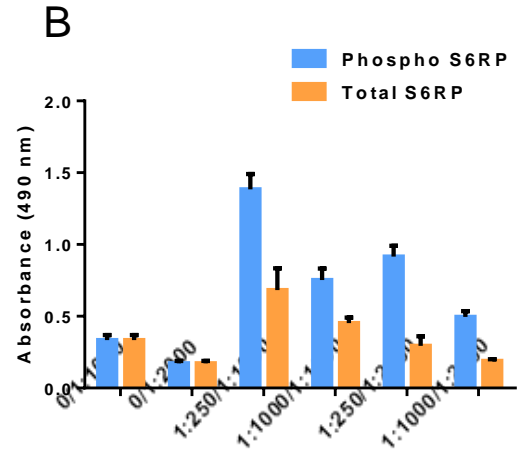
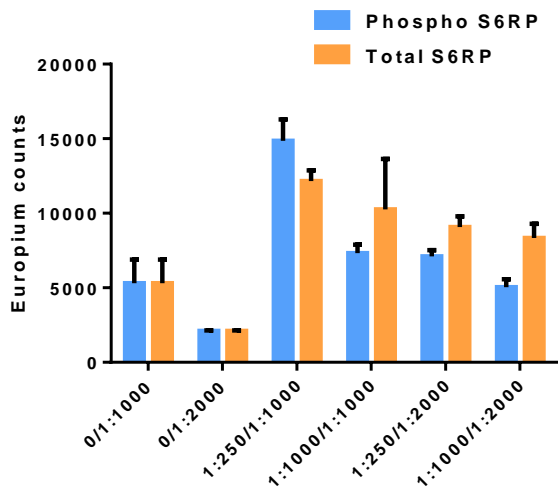


**Figure 3.14. Optimisation of GSK3 $\beta$  cell-based ELISA using Europium and OPD substrates.** Untreated parental ZR-75-1 cells were analysed for their total and phosphorylated GSK3 $\beta$  signalling through A) Europium chelate and B) OPD substrate assays. Summaries of signal-to-noise ratios can be found in C) Various concentrations of primary and secondary antibodies were investigated as a matrix to determine optimal concentrations. X axes shows concentrations of primary antibody/secondary antibody. Data are representative of n=2 independent experiments, and bars represent mean  $\pm$  SD.



| Primary antibody concentration | Secondary antibody concentration | Signal-to-noise ratio |       |
|--------------------------------|----------------------------------|-----------------------|-------|
|                                |                                  | Phospho               | Total |
| 1:250                          | 1:3333                           | 2.8                   | 2.3   |
| 1:1000                         |                                  | 1.4                   | 1.9   |
| 1:250                          | 1:10,000                         | 3.4                   | 4.3   |
| 1:1000                         |                                  | 2.4                   | 4.0   |

| Primary antibody concentration | Secondary antibody concentration | Signal-to-noise ratio |       |
|--------------------------------|----------------------------------|-----------------------|-------|
|                                |                                  | Phospho               | Total |
| 1:250                          | 1:1000                           | 4.1                   | 2.0   |
| 1:1000                         |                                  | 2.3                   | 1.4   |
| 1:250                          | 1:2000                           | 5.3                   | 1.7   |
| 1:1000                         |                                  | 2.9                   | 1.1   |

### **3.3.6. Investigation of PI3K/AKT pathway signalling of resistant sub-clones by cell-based ELISA**

After assay optimisation, cell-based ELISAs were carried out on parental ZR-75-1 and sub-clones B9 and D2. Cells were treated with a range of concentrations of AZD5363 to assess the effect on levels of total and phosphorylated S6RP, and to determine if there are any observable differences in the signals in response to AZD5363 treatment.

Results of cell-based ELISAs probing for S6RP are shown in figure 3.16. These data show a clear decrease in phosphorylation of S6RP in a dose-dependent manner upon treatment with AZD5363. When treated at the highest drug concentration (5  $\mu$ M) levels of phosphorylated S6RP are not notably higher than the background signal. In addition, levels of total S6RP remain relatively consistent throughout the dosing schedule in the parental as well as the two sub-clones. However, the response of the two sub-clones is very similar to that of the parental cell line, as phosphorylation of S6RP decreases at the highest drug concentrations instead of being maintained.

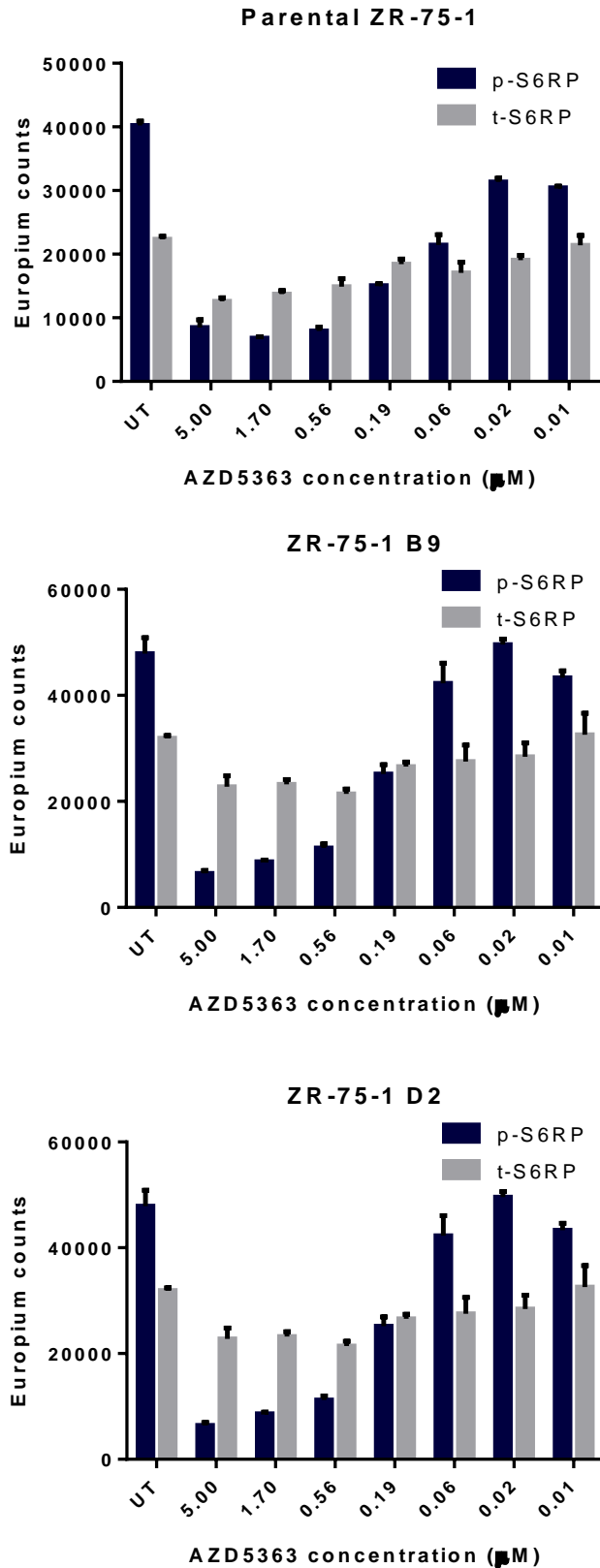


**Figure 3.16. Cell-based ELISA of parental ZR-75-1 and sub-clones B9 and D2.** Cells were plated in a 96-well format and treated with 0.01 μM to 5 μM AZD5363 for 1 hr. Total and phosphorylated S6RP levels were determined using time-resolved fluorescence from europium-labelled antibodies. UT = untreated control. Data are representative of n=2 independent experiments, and bars represent mean ± SD.

## 4.0 Discussion

### 4.1. Introduction

In this research project, the aims were to develop breast cancer sub-clones resistant to the experimental AKT inhibitor AZD5363 and investigate the cellular mechanisms that cause resistance. AZD5363-resistant ovarian carcinoma cell line models have already been established *in vitro* in our laboratory (Akan, Jakubowski, Garrett; unpublished). Therefore, our aim was to determine whether the resistance mechanisms are the same in breast cancer; another disease type in which this inhibitor is being clinically evaluated. Despite there being several AKT inhibitors in clinical trials, little has been done to investigate the potential mechanisms of resistance that may emerge *in vivo*. This study therefore aims to determine the resistance mechanisms to AZD5363 in order to inform potential drug combinations in an effort to limit the acquisition of resistance.

### 4.2. Characterisation of sensitive breast cancer cell lines

From initial preclinical studies into AZD5363 treatment of human cancer cell lines, those derived from breast cancers were seen to be the most sensitive. For example, in one study 64% of breast cancer cell lines were found to be inhibited with a  $GI_{50}$  less than 1  $\mu\text{mol/L}$  and were therefore deemed to be sensitive. On the other hand, cell lines derived from other tissue types such as endometrial, gastric, and prostate cancers showed response rates of just 24% to 33%, and bladder cancer cell lines were deemed to be resistant ( $GI_{50}$  more than 3  $\mu\text{M}$ ). There additionally was an apparent correlation between breast cancer cell lines carrying PI3K/AKT pathway aberrations (such as activating *PIK3CA* mutations or loss of PTEN activity) and AZD5363 sensitivity, as 76% of highly sensitive cell lines carried at least one of these defects (Davies *et al.*, 2012).

The three breast cancer cell lines initially used in this project (T47D, MCF-7 and ZR-75-1) have all been classified as sensitive to AZD5363; particularly T47D and ZR-75-1, which were both determined to have  $GI_{50}$  concentrations of less than 1  $\mu\text{M}$  and were therefore deemed highly sensitive. In this project, the three selected cell lines were found to have AZD5363  $GI_{50}$  concentrations of 0.92  $\mu\text{M}$ , 1.34  $\mu\text{M}$  and 0.05  $\mu\text{M}$  for T47D, MCF-7 and ZR-75-1 respectively.  $GI_{50}$  concentrations were determined by 96-hour sulforhodamine B (SRB) assay, and these values concur with previous characterisation studies which found the ZR-75-1 cell line was most sensitive to AZD5363 treatment, followed by T47D and MCF-7 (Li *et al.*, 2013). Additionally, the presence of PI3K/AKT pathway aberrations and hormone receptor (HR) expression in these cell lines also correlates to sensitivity to AKT inhibition. For example, mutations in *PIK3CA*, the catalytic subunit of PI3K, appear in both T47D and MCF-7. An E545K substitution in the PI3K helical domain appears in T47D, whilst MCF-7

carries an H1047R substitution in the kinase domain. Conversely, ZR-75-1 expresses wild-type *PIK3CA* but does have an L108R substitution mutation in phosphatase and tensin homolog (*PTEN*) leading to weak expression of this protein (Weigelt, Warne and Downward, 2011). Although HER2 is not amplified in this cell line, it has been found to express intermediate levels of this receptor (Ithimakin *et al.*, 2013) – as HER2 expression correlates to high levels of sensitivity to AZD5363, this may also contribute to the highly sensitive nature of this cell line. Furthermore, all three selected cell lines have been found to be positive for both oestrogen receptor and progesterone receptor expression. T47D and MCF-7 are therefore of the luminal A subgroup, characterised by oestrogen and progesterone receptor expression with a concurrent lack of HER2 expression.

Upon  $GI_{50}$  determination assays, it became apparent that T47D did not respond in the same way to AZD5363 as MCF-7 and ZR-75-1. This is because in these cell viability assays, viability did not reach 0% even at the very highest doses of AZD5363. This finding was explored further, as we wanted to know if this was due to induction of cell growth arrest. To achieve this multiple identical SRB plates were produced with one to be fixed every 24 hours, to obtain viability data at multiple timepoints and determine at what point this arrest occurs. This experiment revealed that treatment of T47D with AZD5363 concentrations  $\geq 0.37 \mu\text{M}$  induced growth arrest, regardless of the concentration. Similarly, concentrations  $< 0.37 \mu\text{M}$  slowed growth in a dose-dependent manner, although growth does not stop completely. Propidium iodide (PI) staining and flow cytometry was performed with T47D cells treated with AZD5363 to determine the growth phase in which cytostatic arrest occurs. PI binds to nucleic acids and fluorescence is detected by the flow cytometer; the intensity of the fluorescence is proportional to the nucleic acid content. For example, cells in G2/M phase with 4N DNA will have twice the fluorescence intensity compared to those in G0/G1 phase with 2N DNA. However, there was no significant difference in the percentage of cells in each phase in the treated cells relative to the untreated, despite there being a clear cytostatic effect as seen in figure 3.5. Therefore, it is not likely that growth is being arrested at a single cell cycle checkpoint; if this was the case, there would be a clear accumulation of cells in one population on the histogram. Instead, we hypothesise that T47D cells are arrested in all phases of growth when treated with high concentrations of AZD5363. To investigate this, 5-bromo-2'-deoxyuridine (BrdU) incorporation assays could be used to determine if cell proliferation and flux through the cell cycle are still taking place. This assay measures incorporation of BrdU, a synthetic nucleoside analogue of thymidine, into the DNA. Levels of BrdU can then be detected through fluorescently labelled anti-BrdU antibodies by flow cytometry, to measure DNA synthesis and cell proliferation (Walton *et al.*, 2010). If cells have arrested in all phases, incorporation of BrdU should not occur as

DNA synthesis will not take place. Additionally, to ascertain whether AZD5363 behaves in a more pro-apoptotic manner in MCF-7 and ZR-75-1, Western blots could be carried out to detect levels of apoptotic markers such as cleaved caspase-3 and cleaved PARP. However, these different cellular responses to the drug are consistent with preclinical xenograft studies, in that for some cell lines treatment is only sufficient to cause growth inhibition while in others it can cause tumour regression (Davies *et al.*, 2012).

### **4.3. Generation of resistant cell lines**

The development and characterisation of drug-resistant cancer cell lines is an important step towards identifying the specific resistance mechanisms acquired by patients in the clinic. There is some scepticism over the use of cell line models to investigate resistance mechanisms; however, in some cases *in vitro* models have been successful in predicting acquired resistance in the clinic. For example, three *B-RAF* (V600E)-positive melanoma sub-lines were developed with acquired resistance to the selective *B-RAF* (V600E) inhibitor vemurafenib. Investigation of vemurafenib-resistant patient-derived tumours validated findings from resistant sub-lines generated *in vitro*; this showed that increased expression of platelet-derived growth factor receptor beta (PDGFRβ) is a dominant feature of vemurafenib resistance (Nazarian *et al.*, 2010). Therefore, if similar models can be established for resistance to other drugs such as AZD5363 then this will be of great clinical benefit when predicting resistance mechanisms.

Laboratory methods used in the development of drug-resistant cell lines are frequently overlooked in publications in this field. It is also not uncommon to encounter difficulties in developing cell lines with stable resistance *in vitro*. However, there are several options available in choosing strategies to develop resistance - for example, AZD5363-resistant A2780 ovarian carcinoma cell line was developed through a dose-escalation method. Cells were grown in the presence of 1x the GI<sub>50</sub> concentration of CCT129254 (a precursor of AZD5363) until they reached 70% confluency; these were then passaged and grown in an increased inhibitor concentration. This process was repeated over a six-month period until A2780 cells with acquired resistance to CCT129254/AZD5363 were growing in a final concentration of 20x the GI<sub>50</sub>. These cell line models were developed with 5-fold resistance to CCT129254 (D. Akan, PhD thesis 2015).

Pulsed-selection can be used to more closely mimic the conditions patients would experience during treatment with the aim of being more clinically relevant. In these clinically relevant models, the drug doses are usually consistent with what is given to patients in the hospital setting, and cells can be treated in pulses to mimic specific drug regimens. For example, one study developed H69 small-cell lung cancer cells resistant to cisplatin and

oxaliplatin using drug concentrations between the IC<sub>10</sub> and IC<sub>40</sub>. Additionally, these were administered in pulses either over two hours or four days in order to reproduce the pharmacokinetics and clearance of these similar platinum-based drugs. This study was successful in generating 'regrowth resistance' in this cell line, in which the initial period of growth arrest upon drug treatment had reduced after multiple pulses (Stordal, Davey and Davey, 2006).

Continuous selection and dose-escalation may also be used to generate resistance, producing cell lines being cultured in relatively high drug concentrations that have been gradually increased over time. The resulting sub-lines often have high levels of resistance, and also exhibit a more stable resistance phenotype than sub-lines generated by other methods. Furthermore, these highly resistant cells are more convenient in understanding resistance mechanisms as the molecular changes are often far more pronounced. However, a balance must be sought as very high levels of resistance may be less clinically relevant. One study generated resistance to lapatinib in the inflammatory breast cancer cell line SUM149. This was achieved through chronic exposure of cells to 0.25 µM of a laboratory grade lapatinib analogue (GW583340). After increases in cell death and decreased cell growth, small colonies were cultured until confluence and drug concentration gradually increased to 7.5 µM over a period of 3 months. Dosage of the resistant SUM190 cells with 20 µM lapatinib for 24 hours resulted in only 10-20% increase in cell death, as determined by Annexin/PI staining. This is in comparison to approximately 70-80% cell death and decrease in proliferation in the parental cell line (Aird *et al.*, 2010).

Culturing cancer cell lines in the presence or absence of antibiotics is also another methodologically important choice when developing resistant cell lines. This is because cancer patients are not routinely given antibiotics continually throughout their treatment. Therefore, cells that are continuously cultured in antibiotics may not develop clinically relevant resistance mechanisms (McDermott *et al.*, 2014), and were subsequently not used in routine cell culture in this project.

The methods employed in this project to develop AZD5363-resistant cells were clonal selection combined with chronic exposure to high drug concentration. Cells from breast cancer lines T47D, MCF-7 and ZR-75-1 underwent limiting dilution and were plated in a 96-well format at a concentration of 0.5 cells per well. Alternatively, cells could have been diluted to 1 cell per well – however, plating at 0.5 cells per well decreases the probability of seeding more than one cell in a well and therefore not obtaining a clonal population. After one week of incubation, wells were observed for presence of cell growth, and those containing distinct single colonies of cells were selected for drug treatment. Plates of each

cell line were treated with either 2x, 4x or 10x the  $GI_{50}$  concentration of AZD5363 in that individual cell line. Fresh media and drug was then replaced weekly to ensure nutrient availability for growth, and to ensure cells were chronically exposed to the drug due to breakdown of the molecules over time. However, this process continued over many weeks as cell growth rate was extremely slow. Although this method initially yielded several clonal populations from each cell line, just two were successful in expansion to T25 culture flasks – clones B9 and D2, both from the ZR-75-1 cell line. Interestingly, MCF-7 and T47D cells did not successfully yield resistant sub-clones. The reasoning for this is currently unknown, although it may be due to the relative insensitivity of these cell lines to AZD5363. For example, as MCF-7 has initially a higher  $GI_{50}$  for AZD5363 (1.34  $\mu$ M) compared to ZR-75-1 (0.05  $\mu$ M), this would require MCF-7 cells to grow in a much higher drug concentration which could possibly bring about off-target effects.

One hypothesis for the slow growth rates observed in this method is that cell growth is lack of paracrine inter-cellular signalling due to low cell numbers. Cells of some lines may be less able to grow independently of each other as they are highly reliant on secretion of growth factors by other cells in the population. For example, epidermal growth factor (EGF) can be expressed by cancer cells in culture, ultimately leading to increased cell proliferation, survival, and invasion. This means that survival and proliferation of these cells is linked to availability and secretion of soluble growth factors into the culture medium, and depending on the cell line growth may be impaired when there are only a few cells present in the population. Therefore, when growing clonal populations from single cells, we may be negatively selecting those cells which are less able to grow in the absence of paracrine factors from nearby cells. To overcome this, it is possible to use conditioned media to improve cell growth after limiting dilution. Conditioned media involves collecting media from cells that have been cultured for 24-48 hours, centrifuging and filtering to limit cross-contamination of cells, and mixing with fresh culture media before addition to the chosen cells. This is usually mixed in a 1:1 ratio to retain the secretory factors in the conditioned media, whilst replacing any depleted nutrients such as glucose and glutamate.

Alternatively, cloning rings can be utilised to generate clonal populations. One study used cloning rings to generate clonal subpopulations of a multi-drug resistant (MDR) squamous lung cancer cell line DLKP-A. This involved seeding cells in a 35 mm culture dish at a concentration of 50 cells per dish, feeding with conditioned media and monitoring growth until individual populations reached approximately 50 cells each. Once this size had been reached, cloning rings were placed around each population to create individual chambers from which cells could be trypsinised and seeded into a 96-well plate (Heenan *et al.*, 1997). This method utilised both the benefits of conditioned media and having a larger number of

cells present to allow for paracrine signalling loops. Taken together, these alternative methods described may lead to improved success rates in generating resistant clones.

#### **4.4. Characterisation of resistant sub-clones**

##### **4.4.1. Determining fold-resistance to AZD5363**

After expansion of clonal cell populations into tissue culture flasks, sensitivity to AZD5363 was investigated by SRB assay. The  $GI_{50}$  values for the newly generated clones were compared against that of the parental to calculate their resistance factor. Resistance factors greater than two-fold are usually considered the threshold for classifying a sub-line as resistant. There statistically significant resistance factors for ZR-75-1 clones B9 and D2 of 7.6 and 5.8-fold, respectively. Therefore, resistance to AZD5363 has successfully been generated *in vitro* in this breast cancer cell line.

##### **4.4.2. Resistant sub-clones do not exhibit cross-resistance to other AKT inhibitors**

Resistant sub-clones were also screened by SRB assay for any cross-resistance to other AKT inhibitors currently in phase II clinical trials, GDC0068 and MK2206 (clinicaltrials.gov identifiers NCT02301988, NCT01294306). GDC0068 (ipatasertib) is an orally available potent ATP-competitive pan-AKT inhibitor with relatively high selectivity for AKT, inhibiting only 3 out of 230 kinases by more than 70% at 1  $\mu$ M. It has successfully caused growth stasis and tumour regression as a single agent in mouse xenograft models of tumours with enhanced PI3K/AKT signalling (i.e. activating *PIK3CA* and *PTEN*-null mutations) as well as increasing the anti-tumour activity of drugs such as docetaxel (Lin *et al.*, 2013). Similarly, MK2206 is an orally active allosteric AKT inhibitor, thereby having high selectivity for AKT and high potency against AKT1 and AKT2 isoforms (Hirai *et al.*, 2010). Despite both additional experimental AKT inhibitors potently inhibiting AKT, there was no significant cross-resistance observed between GDC0068 or MK2206 in the AZD5363-resistant clones B9 or D2. These findings are of note as they contrast with the resistance profile of the A2780-5363R ovarian carcinoma sub-line, which does exhibit cross-resistance to inhibition by GDC0068 and MK2206 (D. Akan, PhD thesis 2015). These preliminary findings suggest that the resistance mechanism(s) in the breast cancer sub-clones differ from that of the ovarian sub-line as they do not share cross-resistance to AKT inhibition by other agents. Furthermore, this lack of cross-resistance in sub-clones B9 and D2 suggests that the resistance mechanism is not proximal to AKT, and instead another pathway may be responsible for resistance.

#### **4.4.3. PI3K/AKT signalling is not significantly altered in resistant sub-clones**

To further investigate the hypothesis that the resistance mechanism of the AZD5363-resistant ZR-75-1 sub-clones is not proximal to AKT, Western blots were carried out to probe for components of the key signalling pathways. Firstly, signalling was investigated in untreated parental, B9 and D2 cells (Figure 3.12). However, baseline levels of many signals were consistent between the parental ZR-75-1 and the resistant sub-clones. Phosphorylated Ser473-AKT remains consistently low across ZR-75-1 parental and sub-clones B9 and D2 at a basal level. Phosphorylated GSK3 $\beta$  (a direct downstream substrate of AKT) levels were also maintained between the parental and resistant cells. Levels of phosphorylated and total ERK were investigated as, although not a member of the PI3K/AKT pathway, we were interested to see if MAPK pathway signalling had increased as a resistance mechanism. However, this was not the case as both total and p-ERK remained unchanged in the parental across sub-clones B9 and D2. Additionally, S6RP levels in the resistant cells were also consistent with those of the parental. This is again in contrast to A2780-5363R which shows elevated phosphorylation of S6RP relative to the parental. Furthermore, 4EBP1 levels are not reduced in B9 or D2, differing again from A2780-5363R.

Additionally, a dose-response Western blot with two concentrations of AZD5363 was performed to investigate the effect of drug treatment on PI3K/AKT signalling. ZR-75-1 parental cells as well as sub-clones B9 and D2 were either untreated or exposed to 1x or 3x the GI<sub>50</sub> of AZD5363 for the parental cell line (50 and 150 nM, respectively) for four hours (Figure 3.15). The results of this Western blot revealed that phosphorylation of AKT is increased in the treated cells relative to the untreated. This is a well-documented phenomenon after treatment with AKT-competitive AKT inhibitors. This “paradoxical” hyperphosphorylation was initially thought to occur through homeostatic negative feedback loops; however, subsequent studies have described that occupation of the ATP-binding pocket by similar drugs causes a conformational change in AKT. This change prevents access of phosphatases to the phosphorylated residue Tyr308 in the AKT activation loop, preventing its dephosphorylation and thereby maintaining the kinase in a hyperphosphorylated but catalytically inactive state (Chan *et al.*, 2011). Therefore, this effect is restricted to ATP-competitive AKT inhibitors only – this has not been reported to occur with allosteric inhibitors such as MK2206. Furthermore, other signals remained relatively consistent with those seen in baseline signalling. For example, levels of both total and p-ERK remain consistent across the different cell samples and AZD5363 concentrations.

#### 4.5. Development of cell-based ELISA

Despite Western blotting being the 'gold standard' for investigating protein expression levels for many years, it is still a relatively labour-intensive process which requires previous experience of the technique to yield consistent results. Indeed, protocols are long and contain many steps, increasing the chances of human error affecting the results. Therefore, during this project the possibility of using a cell-based ELISA as a novel high-throughput alternative to Western blotting was explored. Two different labelled antibodies were used for detection; o-phenylenediamine dihydrochloride (OPD) HRP substrate and europium labels. This cell-based ELISA protocol involves seeding of cells in a 96-well format and subsequent fixation and permeabilisation. Fixed cells are blocked in 5% milk to prevent non-specific interactions upon the later addition of primary antibody specific to the target of interest. In these experiments, levels of phosphorylated and total GSK3 $\beta$  and S6K were to be investigated. However, the optimal concentrations of primary and secondary antibodies needed to be determined in order to produce signals with a high signal-to-noise ratio. This was carried out by using a matrix of primary and secondary antibody concentrations for each method. After carrying out these assays, the OPD substrate method was not taken forward for further experiments as the signal-to-noise ratios were very low. The europium chelate had a very high signal-to-noise ratio due to a large Stokes' shift and as well as having a long time period between excitation and emission wavelengths. Ultimately, primary antibody concentrations of 1:1000 and 1:250 were selected for S6RP and GSK3 $\beta$  respectively, and a secondary antibody concentration of 1:3333, as these provided the optimal signal-to-noise ratios.

Cells were incubated overnight in primary antibody at 4°C before washing and further incubation in either A) horseradish peroxidase (HRP) conjugated or B) europium labelled secondary antibody, for one hour. The OPD substrate is converted into a coloured product by HRP, and therefore the results are interpreted colourimetrically, as colour intensity is proportional to the amount of protein present. With the europium-labelled antibodies, a low-pH enhancement solution is added causing dissociation of the Eu<sup>3+</sup> and formation of a highly fluorescent chelate within a protective micelle. Colour or fluorescence can then be determined using a plate reader, with the values generated proportional to the amount of target protein present. Indeed, this method allows for the recording of quantitative, numerical data as opposed to qualitative data as generated by Western blots. Although Western blotting bands can be quantified using densitometry, there are many variables to take into account when doing this and so results are not always reliable. This cell-based ELISA therefore provides a method for high-throughput analysis and relatively fast generation of quantitative data for statistical analysis.

After optimisation of this method was completed, cell-based ELISAs were performed on the parental ZR-75-1 cell line in addition to sub-clones B9 and D2. These cells were treated with a range of concentrations of AZD5363 for one hour, then the assay was performed as previously described. The results of this assay revealed that S6RP phosphorylation decreased in a dose-dependent manner. At the highest AZD5363 concentration (5  $\mu$ M) levels of S6RP phosphorylation was the same as the background signal, showing this assay has a high degree of sensitivity. Additionally, levels of total S6RP remained relatively consistent under each condition. In terms of comparing signalling between parental ZR-75-1 and the resistant sub-clones, there was not a notable change in phosphorylation of S6RP in response to AKT inhibition between the three cell types. This finding therefore contributes to the hypothesis that the resistance mechanism is not proximal to AKT in these sub-clones, as we would expect to see maintenance of S6RP phosphorylation in these cells if that was the case.

Overall, this shows that the cell-based ELISA is likely to be sensitive enough to detect decreases in phosphorylation in response to AKT inhibition; however, it would be beneficial to carry out identical Western blots for a more accurate and direct comparison of the two methods.

#### **4.6. Clinical implications**

Acquired resistance to AKT inhibitors in the clinic has not yet been reported. However, as these inhibitors advance through clinical trials and new experimental drugs are developed resistance may still emerge, as seen with other small molecule inhibitors such as vemurafenib (Nazarian *et al.*, 2010a; Kulkarni *et al.*, 2017).

In the few clinical trials that have reported results, AZD5363 has resulted in some partial responses in patients with tumours that have mutations in either *AKT1* or *PIK3CA* (clinicaltrials.gov identifier NCT01226316). Taken together with results from preclinical studies suggesting monotherapy treatment may lead to some tumour growth inhibition, it is likely that AZD5363 will be more suitable for clinical use when given in combination. This is because combination of AZD5363 with docetaxel, lapatinib, and trastuzumab has been shown to increase their antitumour activity in breast cancer xenografts relative to monotherapy (Davies *et al.*, 2012). Indeed, there are several clinical trials ongoing to determine the effects of AZD5363 when given in combination with paclitaxel or olaparib (clinicaltrials.gov identifiers NCT01625286, NCT02451956, NCT02208375). Furthermore, AZD5363 has potential for use in patients with acquired cisplatin resistance as increased PI3K/AKT pathway activity has been shown to mediate resistance (Fraser, Bai and Tsang,

2008). Use in combination with other drugs is also likely to hinder resistance development as multiple pathways will be targeted concurrently.

Although the resistance mechanism in sub-clones B9 and D2 is still unknown, if further experiments were carried out and the mechanism(s) elucidated, this has the potential to inform possible drug combinations. For example, if a particular kinase is upregulated leading to resistance and there is an inhibitor available for this protein, the two inhibitors could be administered together to limit acquired resistance.

#### **4.7. Proposed resistance mechanism**

The main findings from investigation of the resistant clones are that there is a lack of cross-resistance to other AKT inhibitors GDC0068 and MK2206, and that there is not a significant change in the signalling of the PI3K/AKT pathway. This suggests that the resistance mechanism is not proximal to AKT, and there is another pathway responsible for the resistant phenotype. If this same mechanism of acquired resistance to AZD5363 arises in patients with PI3K/AKT pathway mutations, it may be possible to administer GDC0068 or MK2206 and have the patient still respond to inhibition, due to the lack of AKT inhibitor cross-resistance. We suggest that this may be due to another target of AZD5363; namely PKA. This is because AZD5363 inhibits PKA with an  $IC_{50}$  of 6 nM and is therefore comparable to the potency of AKT2 and AKT3 inhibition. This would account for lack of changes in PI3K/AKT pathway signalling, as it instead could be signals proximal to PKA that have been upregulated. This also concurs with cross-resistance data, as AZD5363 is the only inhibitor of the three that potently inhibits PKA. GDC0068 is >100-fold more selective for AKT than for PKA, with an  $IC_{50}$  of 3.1  $\mu$ M for PKA (Blake *et al.*, 2012), whereas MK2206 has no inhibitory activity against PKA and 250 other kinases (Hirai *et al.*, 2010).

#### **4.8. Future experiments**

To investigate whether PKA activity is responsible for resistance, we can carry out Western blotting in the ZR-75-1 parental cells and resistant sub-clones. For example, antibodies specific for the total and phosphorylated forms of PKA as well as its downstream substrates such as CREB can be used to assess the abundance and activation of these proteins. If the resistance mechanism is proximal to this pathway, then activation of these proteins will be maintained when treated with AZD5363. Additionally, further SRB assays can be carried out with inhibitors of other pathways to check for cross-resistance. For example, an inhibitor of PKA such as PKI 14-22 amide, a cell-permeable peptide potent and specific for PKA ( $K_i$  36 nM) could be used.

Next-generation sequencing techniques such as exome sequencing can also be used to identify mutations that are likely to affect protein function, and may possible candidates for driving resistance. Transcriptomics such as RNA sequencing can also be used to measure gene expression of these candidates to determine if there are differences in expression between ZR-75-1 parental cells and the resistant sub-clones. If differences are identified, then these targets can be further investigated by Western blotting to determine their role in resistance.

As previously mentioned, measurement of DNA synthesis through detection of BrdU incorporation in T47D cells would help to further investigate the cytostatic effect that AZD5363 is having on these cells. This technique would determine whether T47D cells are arresting in all cell cycle phases upon AZD5363 treatment.

#### **4.9. Conclusions**

To conclude, we have developed two AZD5363-resistant sub-clones of the breast cancer cell line ZR-75-1, named B9 and D2. These exhibit a 7.6 and 5.8-fold resistance to AZD5363, respectively. However, in contrast to the A2780-5363R ovarian carcinoma sub-line, there is no significant cross-resistance to AKT inhibitors GDC0068 or MK2206. Furthermore, there are no significant changes in signalling of the PI3K/AKT pathway were observed in the resistant clones. Taken together, although the exact resistance mechanism is as yet unknown, our data suggests that the resistance mechanism is not proximal to AKT. We suggest that resistance may be due to changes in PKA signalling as PKA is inhibited by AZD5363 but not GDC0068 or MK2206, thus providing a possible explanation for the lack of AKT inhibitor cross-resistance. Ultimately, this is an issue which warrants further investigation.

## References

- Addie, M. *et al.* (2013) 'Discovery of 4-amino-N-[(1S)-1-(4-chlorophenyl)-3-hydroxypropyl]-1-(7H-pyrrolo[2,3-d]pyrimidin-4-yl)piperidine-4-carboxamide (AZD5363), an orally bioavailable, potent inhibitor of Akt kinases', *Journal of Medicinal Chemistry*, 56(5), pp. 2059–2073. doi: 10.1021/jm301762v.
- Aird, K. M. *et al.* (2010) 'X-linked inhibitor of apoptosis protein inhibits apoptosis in inflammatory breast cancer cells with acquired resistance to an ErbB1/2 tyrosine kinase inhibitor.', *Molecular cancer therapeutics*, 9(5), pp. 1432–42. doi: 10.1158/1535-7163.MCT-10-0160.
- Andjelkovic, M. *et al.* (1996) 'Activation and phosphorylation of a pleckstrin homology domain containing protein kinase (RAC-PK/PKB) promoted by serum and protein phosphatase inhibitors (signal transduction/mitogenic activation/phosphatase inhibitors/phosphatidylinositol 3-kinase)', 93, pp. 5699–5704.
- Banerji, U. *et al.* (2015) *A pharmacokinetically (PK) and pharmacodynamically (PD) driven phase I trial of the pan-AKT inhibitor AZD5363 with expansion cohorts in PIK3CA mutant breast and gynecological cancers.*, *J Clin Oncol* 33, 2015 (suppl; abstr 2500).
- Barrie, S. E. *et al.* (2003) 'High-throughput screening for the identification of small-molecule inhibitors of retinoblastoma protein phosphorylation in cells', *Analytical Biochemistry*, 320(1), pp. 66–74. doi: 10.1016/S0003-2697(03)00349-X.
- Blake, J. F. *et al.* (2012) 'Discovery and preclinical pharmacology of a selective ATP-competitive Akt inhibitor (GDC-0068) for the treatment of human tumors', *Journal of Medicinal Chemistry*, 55(18), pp. 8110–8127. doi: 10.1021/jm301024w.
- Brunet, A. *et al.* (2001) 'Protein kinase SGK mediates survival signals by phosphorylating the forkhead transcription factor FKHRL1 (FOXO3a)', *Molecular and cellular biology*, 21(3), pp. 952–65. doi: 10.1128/MCB.21.3.952-965.2001.
- Cardone, M. H. (1998) 'Regulation of Cell Death Protease Caspase-9 by Phosphorylation', *Science*, 282(5392), pp. 1318–1321. doi: 10.1126/science.282.5392.1318.
- Carpten, J. D. *et al.* (2007) 'ARTICLES A transforming mutation in the pleckstrin homology domain of AKT1 in cancer'. doi: 10.1038/nature05933.
- Carracedo, A. and Pandolfi, P. P. (2008) 'The PTEN-PI3K pathway: of feedbacks and cross-talks.', *Oncogene*, 27(41), pp. 5527–41. doi: 10.1038/onc.2008.247.
- Ceilley, E. *et al.* (2005) 'Radiotherapy for invasive breast cancer in North America and Europe: Results of a survey', *International Journal of Radiation Oncology Biology Physics*, pp. 365–373. doi: 10.1016/j.ijrobp.2004.05.069.
- Chan, T. O. *et al.* (2011) 'Resistance of Akt kinases to dephosphorylation through ATP-dependent conformational plasticity', *Proceedings of the National Academy of Sciences*, 108(46), pp. E1120–E1127. doi: 10.1073/pnas.1109879108.
- Cheng, J. Q. *et al.* (2005) 'The Akt/PKB pathway: molecular target for cancer drug discovery.', *Oncogene*, 24(50), pp. 7482–7492. doi: 10.1038/sj.onc.1209088.

- Crafter, C. *et al.* (2015) 'Combining AZD8931, a novel EGFR/HER2/HER3 signalling inhibitor, with AZD5363 limits AKT inhibitor induced feedback and enhances antitumour efficacy in HER2-amplified breast cancer models', *International Journal of Oncology*, 47(2), pp. 446–454. doi: 10.3892/ijo.2015.3062.
- Crouthamel, M. C. *et al.* (2009) 'Mechanism and management of AKT inhibitor-induced hyperglycemia', *Clinical Cancer Research*, 15(1), pp. 217–225. doi: 10.1158/1078-0432.CCR-08-1253.
- Datta, S. R., Brunet, A. and Greenberg, M. E. (1999) 'Cellular survival: A play in three acts', *Genes and Development*, pp. 2905–2927. doi: 10.1101/gad.13.22.2905.
- Davies, B. R. *et al.* (2012) 'Preclinical pharmacology of AZD5363, an inhibitor of AKT: pharmacodynamics, antitumor activity, and correlation of monotherapy activity with genetic background.', *Molecular cancer therapeutics*, 11(4), pp. 873–87. doi: 10.1158/1535-7163.MCT-11-0824-T.
- Davies, B. R. *et al.* (2015) 'Tumors with AKT1E17K Mutations Are Rational Targets for Single Agent or Combination Therapy with AKT Inhibitors.', *Molecular cancer therapeutics*, 14(11), pp. 2441–51. doi: 10.1158/1535-7163.MCT-15-0230.
- Dawood, S. *et al.* (2010) 'Prognosis of women with metastatic breast cancer by HER2 status and trastuzumab treatment: An institutional-based review', *Journal of Clinical Oncology*, 28(1), pp. 92–98. doi: 10.1200/JCO.2008.19.9844.
- Diehl, J. A. *et al.* (1998) 'Glycogen synthase kinase-3 $\beta$  regulates cyclin D1 proteolysis and subcellular localization'.
- Dummler, B. and Hemmings, B. A. (2007) 'Physiological roles of PKB/Akt isoforms in development and disease'.
- Elston, C. W. and Ellis, I. O. (2002) 'Pathological prognostic factors in breast cancer. I. The value of histological grade in breast cancer: experience from a large study with long-term follow-up.', *Histopathology*, 41(3A), pp. 154–161. doi: 10.1111/j.1365-2559.1991.tb00229.x.
- Ferlay, J. *et al.* (2015) 'Cancer incidence and mortality worldwide: Sources, methods and major patterns in GLOBOCAN 2012', *International Journal of Cancer*, 136(5), pp. E359–E386. doi: 10.1002/ijc.29210.
- Fraser, M., Bai, T. and Tsang, B. K. (2008) 'Akt promotes cisplatin resistance in human ovarian cancer cells through inhibition of p53 phosphorylation and nuclear function.', *International journal of cancer. Journal international du cancer*, 122(3), pp. 534–46. doi: 10.1002/ijc.23086.
- Fritsch, C. *et al.* (2014) 'Characterization of the novel and specific PI3K $\alpha$  inhibitor NVP-BYL719 and development of the patient stratification strategy for clinical trials', *Molecular Cancer Therapeutics*, 13(5), pp. 1117–1129. doi: 10.1158/1535-7163.mct-13-0865.
- Hanahan, D. and Weinberg, R. A. (2000) 'The hallmarks of cancer.', *Cell*, 100(1), pp. 57–70. doi: 10.1007/s00262-010-0968-0.
- Heenan, M. *et al.* (1997) 'Isolation from a human MDR lung cell line of multiple clonal subpopulations which exhibit significantly different drug resistance'.

*International Journal of Cancer*, 71(5), pp. 907–915. doi: 10.1002/(SICI)1097-0215(19970529)71:5<907::AID-IJC33>3.0.CO;2-1.

Hennessy, B. T. *et al.* (2005) 'Exploiting the PI3K/AKT pathway for cancer drug discovery.', *Nature reviews. Drug discovery*, 4(December), pp. 988–1004. doi: 10.1038/nrd1902.

Hirai, H. *et al.* (2010) 'MK-2206, an allosteric Akt inhibitor, enhances antitumor efficacy by standard chemotherapeutic agents or molecular targeted drugs in vitro and in vivo.', *Molecular cancer therapeutics*, 9(7), pp. 1956–67. doi: 10.1158/1535-7163.MCT-09-1012.

Ithimakin, S. *et al.* (2013) 'HER2 drives luminal breast cancer stem cells in the absence of HER2 amplification: Implications for efficacy of', *Cancer Research*, 73(5), pp. 1635–1646. doi: 10.1158/0008-5472.CAN-12-3349.

Kampa, M. *et al.* (2004) 'Antiproliferative and apoptotic effects of selective phenolic acids on T47D human breast cancer cells: potential mechanisms of action', *Breast Cancer Research*, 6(2), p. R63. doi: 10.1186/bcr752.

Kobayashi, T. and Cohen, P. (1999) 'Activation of serum- and glucocorticoid-regulated protein kinase by agonists that activate phosphatidylinositol 3-kinase is mediated by 3-phosphoinositide-dependent protein kinase-1 (PDK1) and PDK2', *The Biochemical journal*, 339, pp. 319–328. doi: 10.1042/0264-6021:3390319.

Kulkarni, A. *et al.* (2017) 'BRAF fusion as a novel mechanism of acquired resistance to vemurafenib in BRAF V600E mutant melanoma', *Clinical Cancer Research*, p. clincanres.0758.2016. doi: 10.1158/1078-0432.CCR-16-0758.

Kumar, a., Voet, a. and Zhang, K. Y. J. (2012) 'Fragment Based Drug Design: From Experimental to Computational Approaches', *Current Medicinal Chemistry*, 19(30), pp. 5128–5147. doi: 10.2174/092986712803530467.

Li, J. *et al.* (2013) 'The AKT inhibitor AZD5363 is selectively active in PI3KCA mutant gastric cancer, and sensitizes a patient-derived gastric cancer xenograft model with PTEN loss to Taxotere.', *Journal of translational medicine*, 11, p. 241. doi: 10.1186/1479-5876-11-241.

Lin, J. *et al.* (2013) 'Targeting activated Akt with GDC-0068, a novel selective Akt inhibitor that is efficacious in multiple tumor models', *Clinical Cancer Research*, 19(7), pp. 1760–1772. doi: 10.1158/1078-0432.CCR-12-3072.

Liu, P. *et al.* (2009) 'Targeting the phosphoinositide 3-kinase pathway in cancer.', *Nature reviews. Drug discovery*, 8(8), pp. 627–44. doi: 10.1038/nrd2926.

Maira, S. M. *et al.* (2012) 'Identification and characterization of NVP-BKM120, an orally available pan-class I PI3-kinase inhibitor', *Molecular Cancer Therapeutics*, 11(2), pp. 317–328. doi: 10.1158/1535-7163.mct-11-0474.

Maxwell Parkin, D. *et al.* (2001) 'Estimating the world cancer burden: Globocan 2000', *International Journal of Cancer*, pp. 153–156. doi: 10.1002/ijc.1440.

McDermott, M. *et al.* (2014) 'In vitro Development of Chemotherapy and Targeted Therapy Drug-Resistant Cancer Cell Lines: A Practical Guide with Case Studies.', *Frontiers in oncology*, 4(March), p. 40. doi: 10.3389/fonc.2014.00040.

- McHardy, T. *et al.* (2010) 'Discovery of 4-amino-1-(7H-pyrrolo[2,3-d]pyrimidin-4-yl)piperidine-4-carboxamides as selective, orally active inhibitors of protein kinase B (Akt)', *J.Med.Chem.*, 53(1520–4804 (Electronic)), pp. 2239–2249. doi: 10.1021/jm901788j.
- Moasser, M. M. (2007) 'The oncogene HER2: its signaling and transforming functions and its role in human cancer pathogenesis.', *Oncogene*, 26(45), pp. 6469–87. doi: 10.1038/sj.onc.1210477.
- Nagata, Y. *et al.* (2004) 'PTEN activation contributes to tumor inhibition by trastuzumab, and loss of PTEN predicts trastuzumab resistance in patients', *Cancer Cell*, 6(2), pp. 117–127. doi: 10.1016/j.ccr.2004.06.022.
- Nandini, D., Pradip, D. and Brian, L.-J. (2017) 'PI3K-AKT-mTOR inhibitors in breast cancers: From tumor cell signaling to clinical trials', *Pharmacology & Therapeutics*. doi: 10.1016/j.pharmthera.2017.02.037.
- Nave, B. T. *et al.* (1999) 'Mammalian target of rapamycin is a direct target for protein kinase B : identification of a convergence point for opposing effects of insulin and amino-acid deficiency on protein translation', *Biochem. J*, 344, pp. 427–431.
- Nazarian, R. *et al.* (2010a) 'Melanomas acquire resistance to B-RAF(V600E) inhibition by RTK or N-RAS upregulation.', *Nature*, 468(7326), pp. 973–7. doi: 10.1038/nature09626.
- Nazarian, R. *et al.* (2010b) 'Melanomas acquire resistance to B-RAF(V600E) inhibition by RTK or N-RAS upregulation.', *Nature*, 468(7326), pp. 973–7. doi: 10.1038/nature09626.
- O'Neill, A. K., Niederst, M. J. and Newton, A. C. (2013) 'Suppression of survival signalling pathways by the phosphatase PHLPP', *FEBS Journal*, pp. 572–583. doi: 10.1111/j.1742-4658.2012.08537.x.
- O'Reilly, K. E. *et al.* (2006) 'mTOR inhibition induces upstream receptor tyrosine kinase signaling and activates Akt', *Cancer Research*, 66(3), pp. 1500–1508. doi: 10.1158/0008-5472.CAN-05-2925.
- Okuzumi, T. *et al.* (2009) 'Inhibitor hijacking of Akt activation', *Nat Chem Biol*, 5(7), pp. 484–493. doi: 10.1038/nchembio.183.
- Parkin, D. M. *et al.* (2005) 'Global Cancer Statistics, 2002', *CA: A Cancer Journal for Clinicians*, 55(2), pp. 74–108. doi: 10.3322/canjclin.55.2.74.
- Saal, L. H. *et al.* (2005) 'PIK3CA mutations correlate with hormone receptors, node metastasis, and ERBB2, and are mutually exclusive with PTEN loss in human breast carcinoma', *Cancer Research*, 65(7), pp. 2554–2559. doi: 10.1158/0008-5472-CAN-04-3913.
- Samuels, Y. *et al.* (2004) 'Brevia: high frequency of mutations of the PIK3Ca gene in human cancers', *Science*, 304(5670), p. 554. doi: 10.1126/science.1096502.
- Sarbassov, D. D. *et al.* (2005) 'Phosphorylation and regulation of Akt/PKB by the rictor-mTOR complex.', *Science (New York, N. Y.)*, 307(5712), pp. 1098–101. doi: 10.1126/science.1106148.

- Shi, H. *et al.* (2014) 'Acquired resistance and clonal evolution in melanoma during BRAF inhibitor therapy', *Cancer Discovery*, 4(1). doi: 10.1158/2159-8290.CD-13-0642.
- Siegel, R. *et al.* (2014) 'Cancer statistics, 2014', *CA: a cancer journal for clinicians*, 64(1), pp. 9–29. doi: 10.3322/caac.21208.
- Sommer, E. M. *et al.* (2013) 'Elevated SGK1 predicts resistance of breast cancer cells to Akt inhibitors.', *The Biochemical journal*, 452(3), pp. 499–508. doi: 10.1042/BJ20130342.
- Spaans, J. N. and Goss, G. D. (2014) 'Drug resistance to molecular targeted therapy and its consequences for treatment decisions in non-small-cell lung cancer.', *Frontiers in oncology*, 4(July), p. 190. doi: 10.3389/fonc.2014.00190.
- Stambolic, V. *et al.* (1998) 'Negative regulation of PKB/Akt-dependent cell survival by the tumor suppressor PTEN', *Cell*, 95(1), pp. 29–39. doi: 10.1016/S0092-8674(00)81780-8.
- Stemke-Hale, K. *et al.* (2008) 'An integrative genomic and proteomic analysis of PIK3CA, PTEN, and AKT mutations in breast cancer', *Cancer Research*, 68(15), pp. 6084–6091. doi: 10.1158/0008-5472.CAN-07-6854.
- Stordal, B. K., Davey, M. W. and Davey, R. A. (2006) 'Oxaliplatin induces drug resistance more rapidly than cisplatin in H69 small cell lung cancer cells', *Cancer Chemotherapy and Pharmacology*, 58(2), pp. 256–265. doi: 10.1007/s00280-005-0148-7.
- Stottrup, C., Tsang, T. and Chin, Y. R. (2016) 'Upregulation of AKT3 Confers Resistance to the AKT Inhibitor MK2206 in Breast Cancer.', *Molecular cancer therapeutics*, 15(8), pp. 1964–74. doi: 10.1158/1535-7163.MCT-15-0748.
- Swanton, C. (2012) 'Intratumor heterogeneity: Evolution through space and time', *Cancer Research*, pp. 4875–4882. doi: 10.1158/0008-5472.CAN-12-2217.
- Tamura, K. *et al.* (2016) 'Safety and tolerability of AZD5363 in Japanese patients with advanced solid tumors', *Cancer Chemotherapy & Pharmacology*. Springer Berlin Heidelberg, 77(4), pp. 787–795. doi: <http://dx.doi.org/10.1007/s00280-016-2987-9>.
- Thomas, H. and Coley, H. M. (2003) 'Overcoming multidrug resistance in cancer: An update on the clinical strategy of inhibiting P-glycoprotein', *Cancer Control*, pp. 159–165. doi: 10.1358/dof.2009.034.01.1317151.
- Veronesi, U. *et al.* (2009) 'Rethinking TNM: A breast cancer classification to guide to treatment and facilitate research', *Breast Journal*, 15(3), pp. 291–295. doi: 10.1111/j.1524-4741.2009.00719.x.
- Walton, M. I. *et al.* (2010) 'The Preclinical Pharmacology and Therapeutic Activity of the Novel CHK1 Inhibitor SAR-020106', *Molecular Cancer Therapeutics*, 9(1), pp. 89–100. doi: 10.1158/1535-7163.MCT-09-0938.
- Weigelt, B., Warne, P. H. and Downward, J. (2011) 'PIK3CA mutation, but not PTEN loss of function, determines the sensitivity of breast cancer cells to mTOR inhibitory drugs.', *Oncogene*, 30(29), pp. 3222–33. doi: 10.1038/onc.2011.42.

Yang, Q. *et al.* (2015) 'Idelalisib: First-in-class PI3K delta inhibitor for the treatment of chronic lymphocytic leukemia, small lymphocytic leukemia, and follicular lymphoma', *Clinical Cancer Research*, 21(7), pp. 1537–1542. doi: 10.1158/1078-0432.CCR-14-2034.

Yu, H. A. *et al.* (2013) 'Analysis of tumor specimens at the time of acquired resistance to EGFR-TKI therapy in 155 patients with EGFR-mutant lung cancers', *Clinical Cancer Research*, 19(8), pp. 2240–2247. doi: 10.1158/1078-0432.CCR-12-2246.

Yu, H., Littlewood, T. and Bennett, M. (2015) 'Akt isoforms in vascular disease'. doi: 10.1016/j.vph.2015.03.003.

Zhang, Y. *et al.* (2016) 'A novel AKT inhibitor, AZD5363, inhibits phosphorylation of AKT downstream molecules, and activates phosphorylation of mTOR and SMG-1 dependent on the liver cancer cell type', *Oncology Letters*, 11(3), pp. 1685–1692. doi: 10.3892/ol.2016.4111.